Materials Science at the ESRF

What is (Structural) Materials Science?

- Effect of structure on materials properties
- In particular, micro and nano-structure
- more particularly, defects in that structure

Materials Science = Real systems

- Spatial resolution
- In operando conditions (time resolution)
- Characterization of heterogeneity

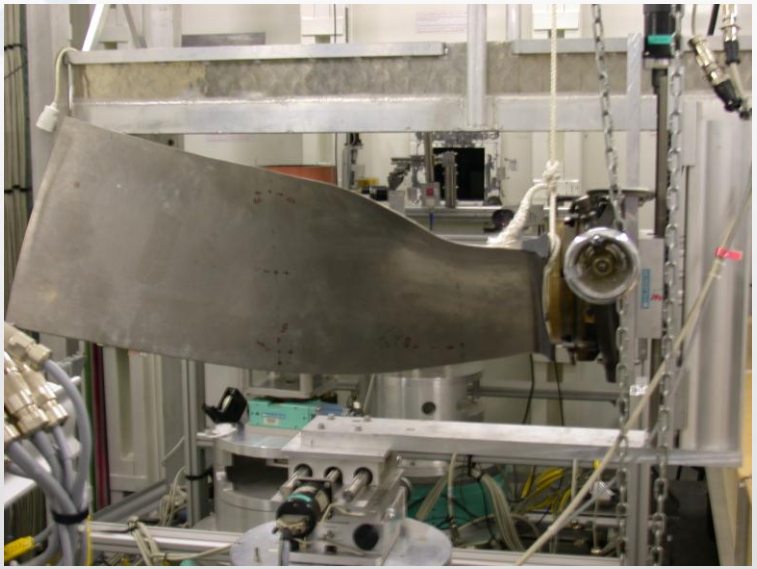

Strain distribution in a jet engin turbine blade

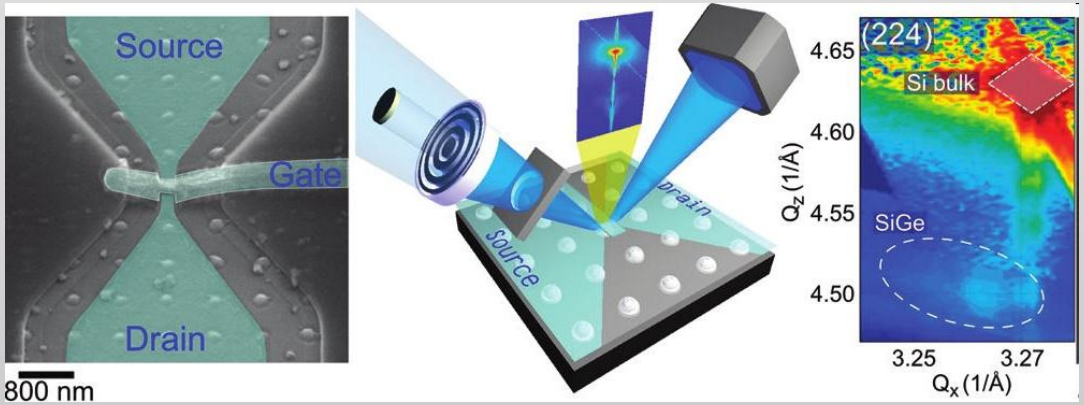

X-ray Nano-diffraction on a Single SiGe Quantum Dot inside a Functioning Field-Effect Transistor (*N. Hrauda et al. Nano Letters 2011*)

Strain

Strain : $(a_{nano-structure} - a_{Bulk}) / a_{Bulk}$ [%]

... intimately related to **physical properties & functionality** of nano-materials (optical, electronic, magnetic, mechanical...)

Its origin:

epitaxial growth on a substrate

surrounding matrix

interfaces with other materials or phases (core-shell, stacking faults ...)

shaping procedures: cutting, etching, rolling

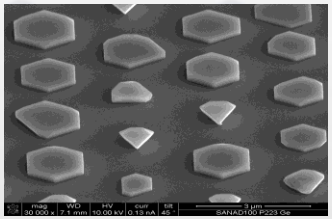

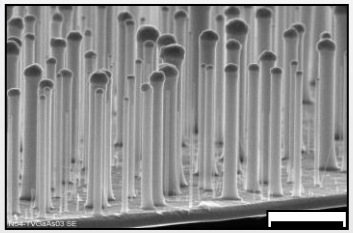

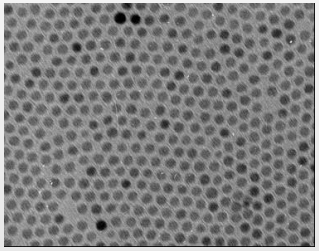

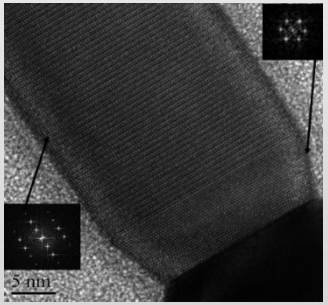

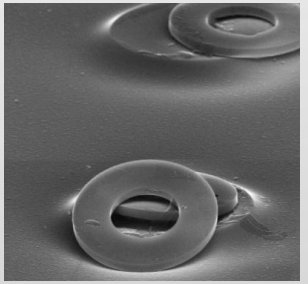

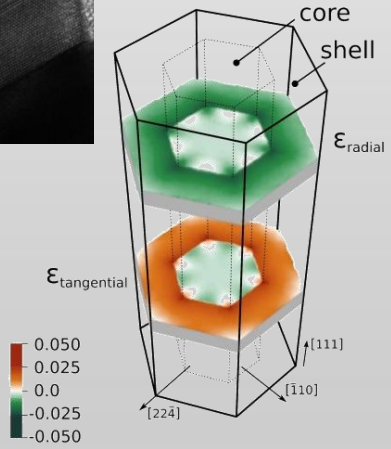

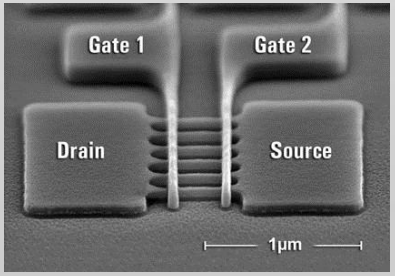

ESRF Structure of Materials

Surfaces, Interfaces and Bulk

Techniques: X-Ray Diffraction, Scattering, Imaging, etc.

ID01	ID03	ID15	ID11	ID31
Surface diffraction		Buried interfaces Liquid surfaces Bulk diffraction Fast tomography Diffraction tomography	Nano beams Grain mapping Chemical crystallography Fast powder diffraction	High resolution powder diffraction 6 – 62 keV
Coherent diffraction imaging Nano beams	Catalysis Surface scattering			

Total Nano-Characterisation

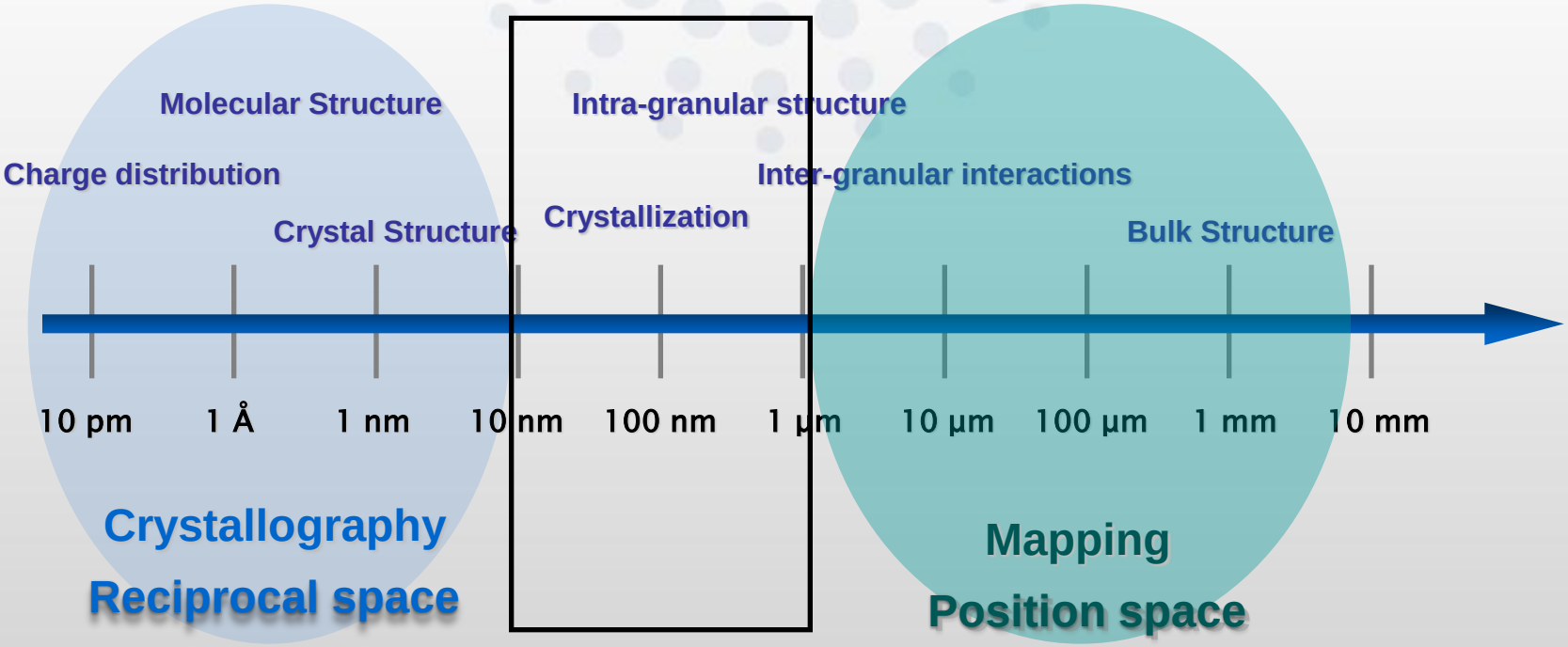

Scale Gap:
New Science

Length Scale and technique

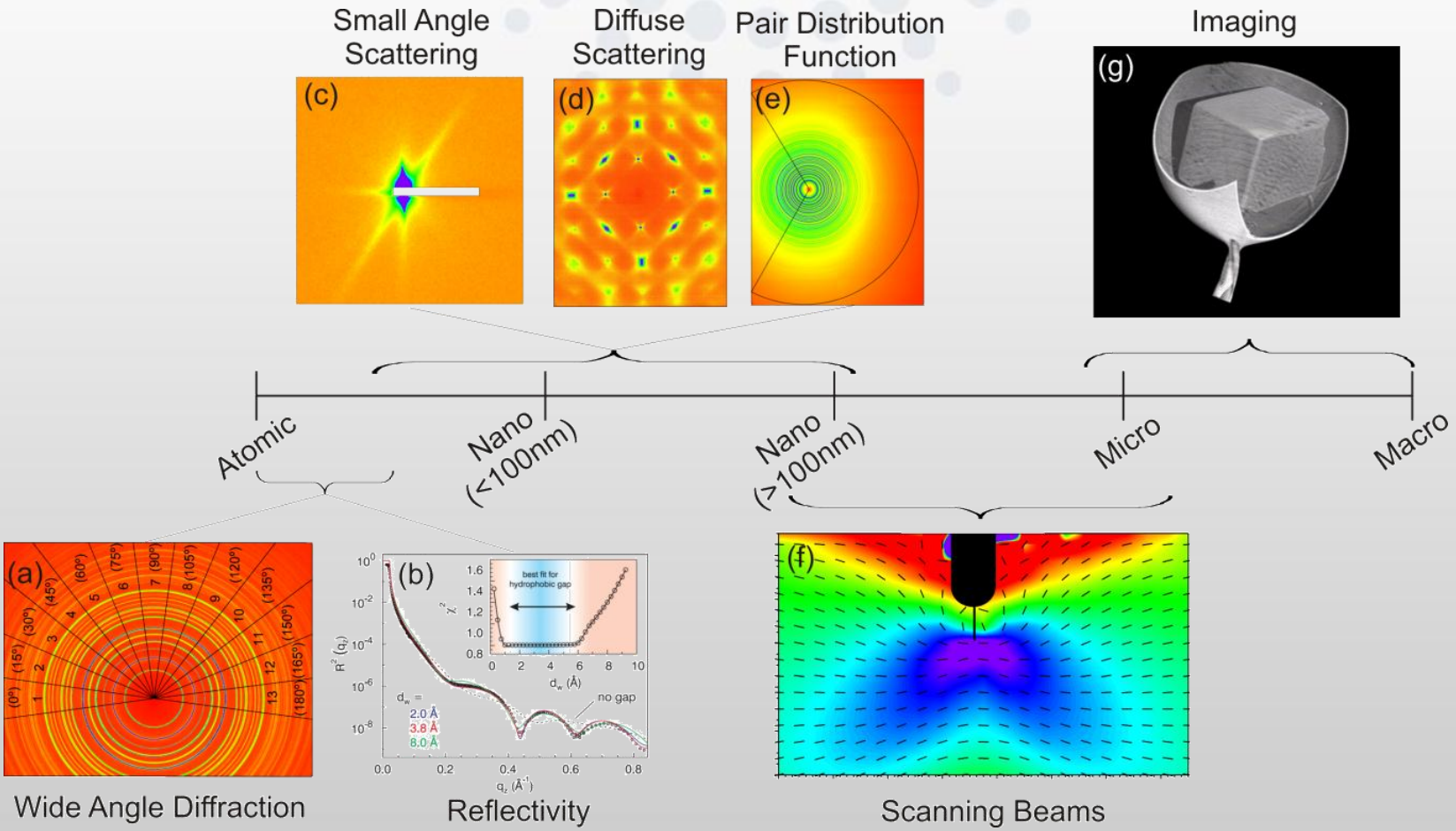

Reciprocal Space

Crystallography : Easy

Amorphous: Getting Easy

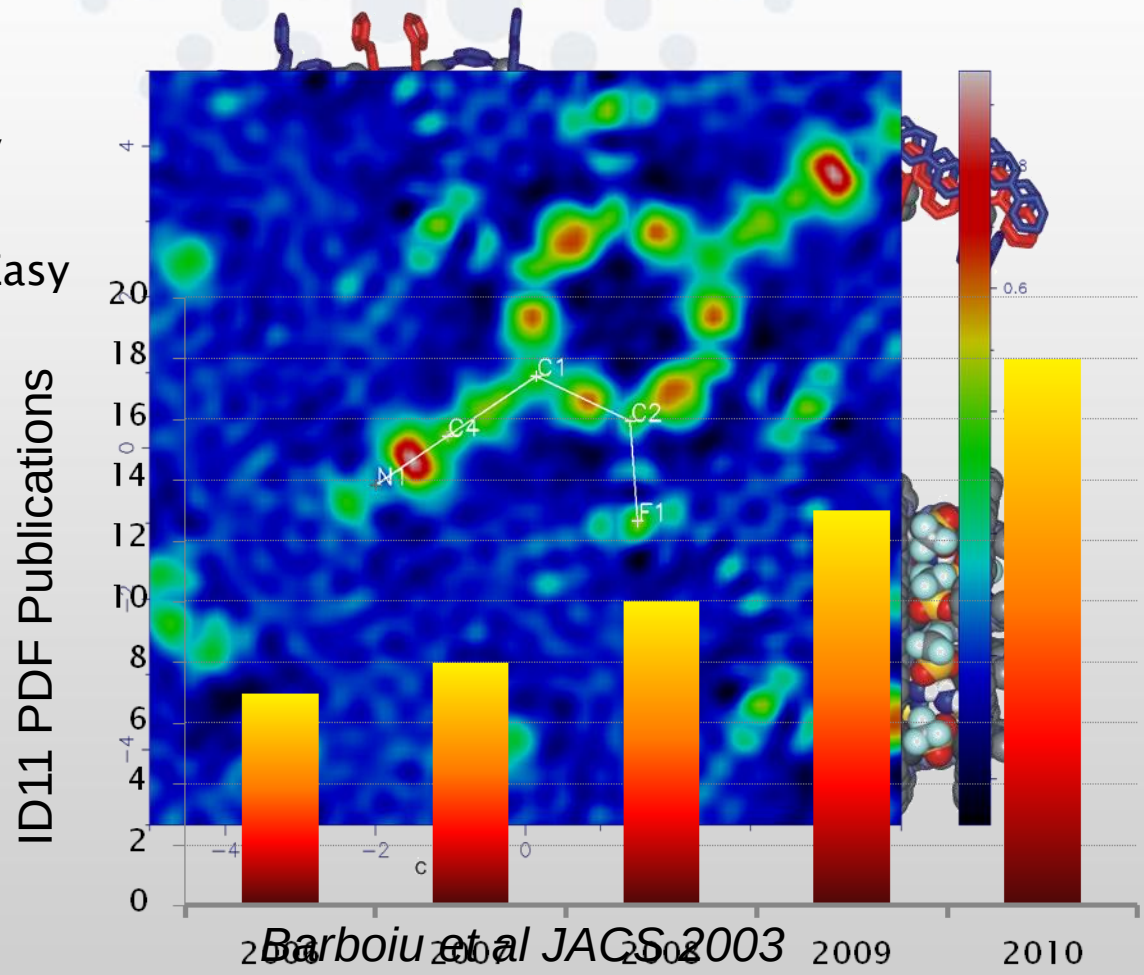

Barboiu et al JACS 2003

High Resolution Powder diffraction (ID31): Structure solution for a metal-organic framework (MIL-100).

a = 72.9 Å	V = 387,420 Å^3
Fd-3*m*	Z = 68 atoms

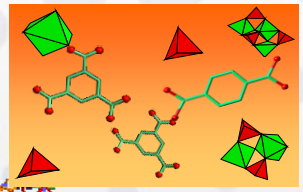

Structure solution from computer simulations

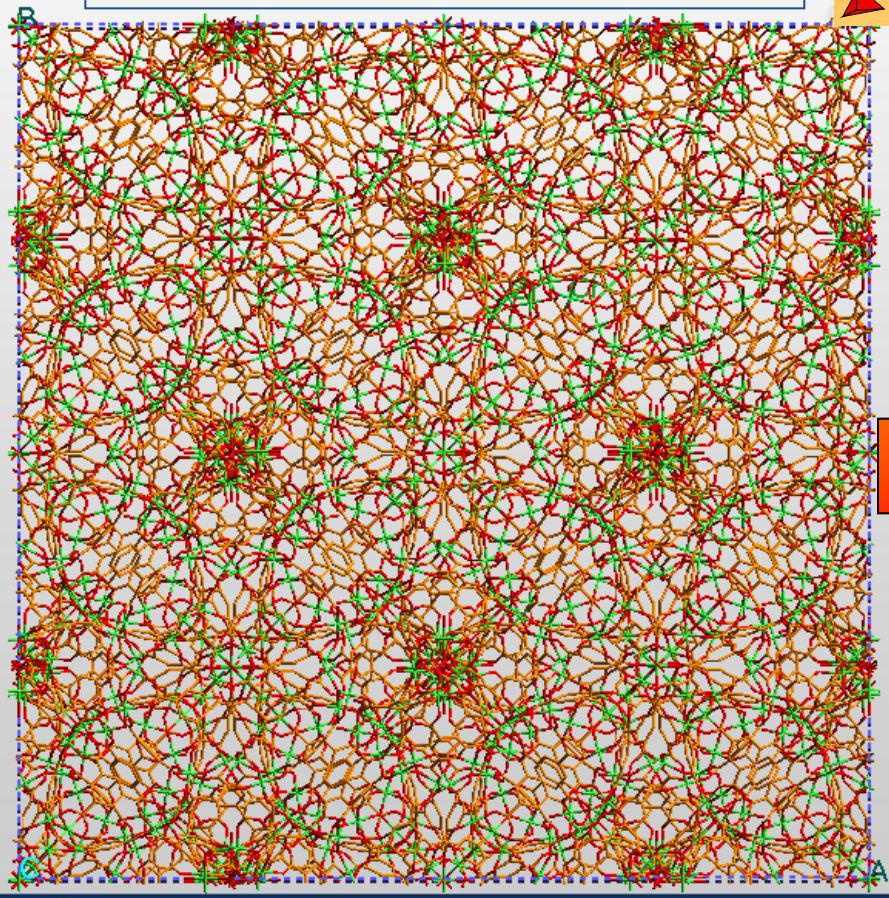

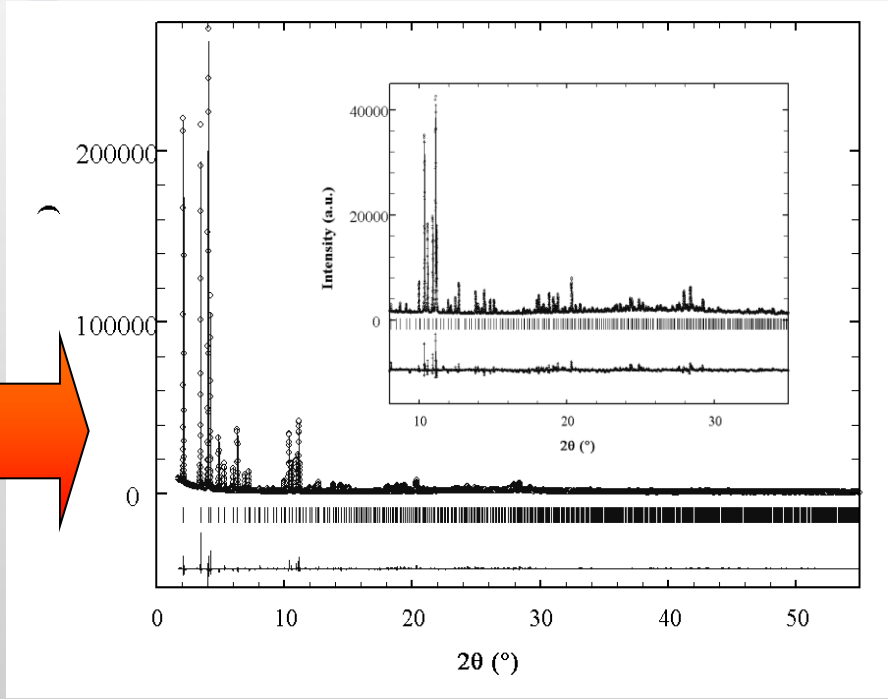

G. Férey et al. Angewandte Chem. 43, 2, (2004)

The computationally designed trimeric building block chelated by three carboxylic functions

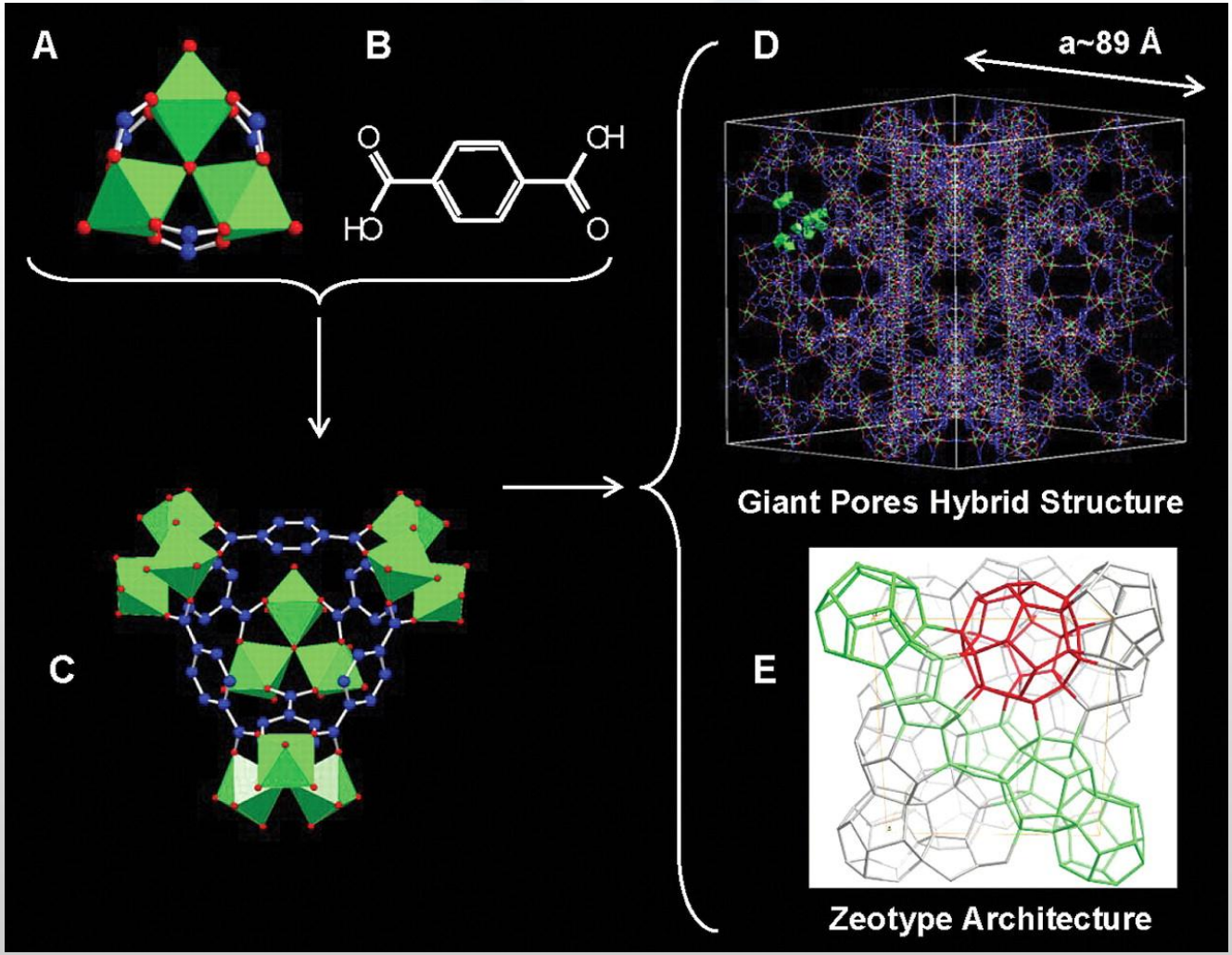

G. Férey et al., Science 309, 2040 -2042 (2005)

Published by AAAS

PDF analysis (ID11, ID15, ID31)

Pair Distribution Function analysis allows atomic scale information to be obtained in even crystallographically-challenged materials, e.g.

- glasses,
- quasicrystals,
- nanoparticles, nanocrystals,
- disordered and heavily defective materials,
- aperiodic materials, etc.

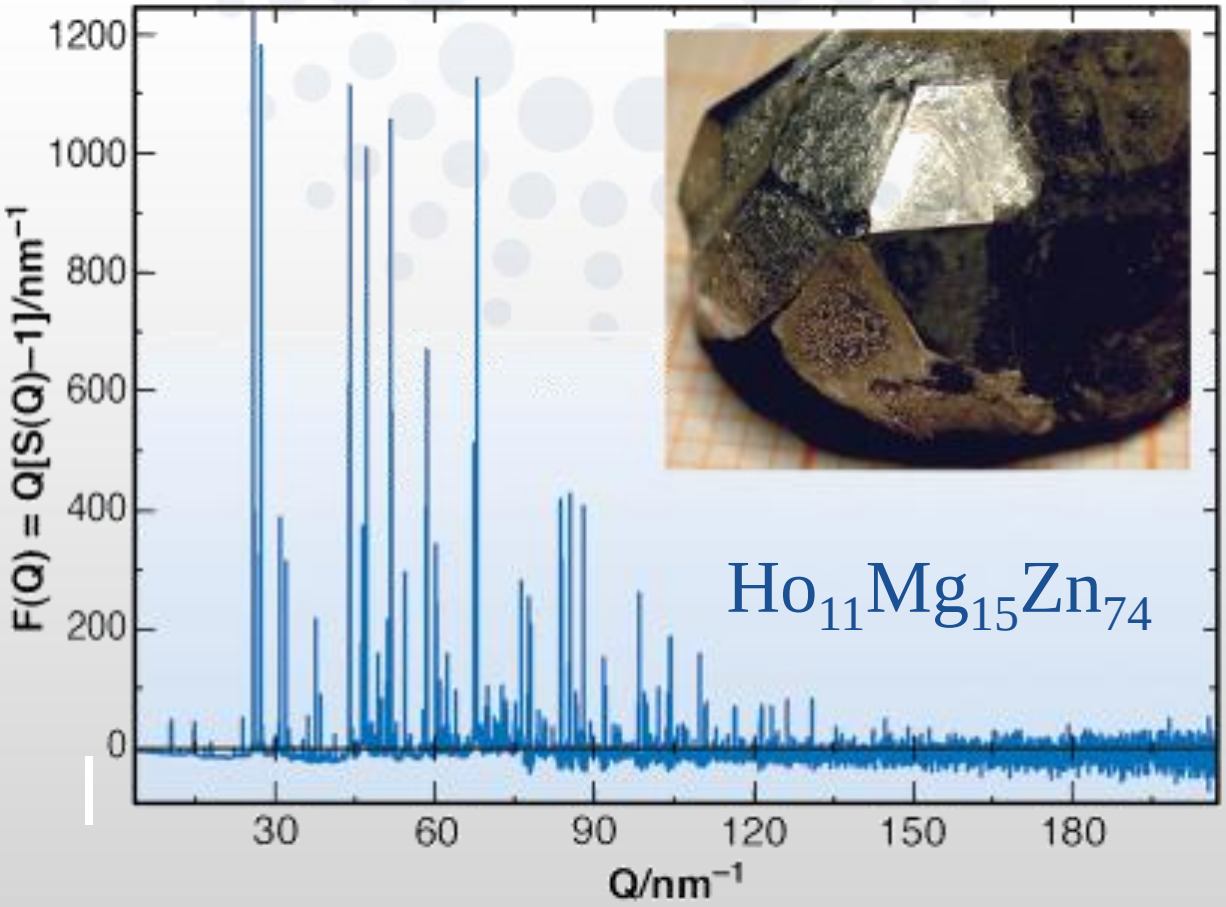

S. Brühne *et al.*, Z. Krist. 220 (2005).

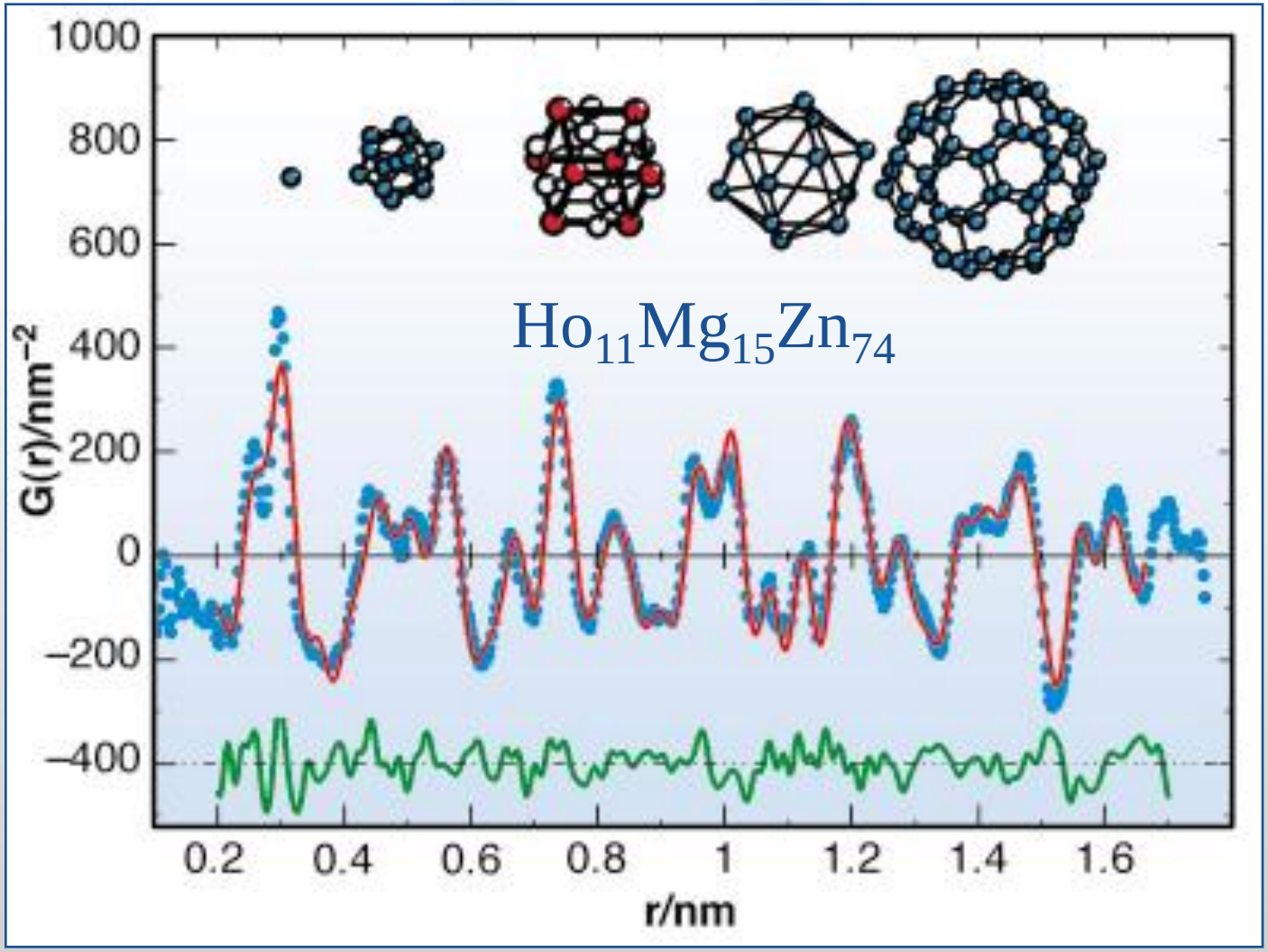

Real-space fit of model

Multicrystal Crystallography (ID11)

Get complete data sets with small rotations:

- Fast
- Low dose

Sample preparation is “straightforward”

- Polycrystalline samples from everyday life
- Samples changing during the experiment

Want techniques to be usable by anyone

Example:

- Photochemistry

Photochemisty

Work of J Davaasambuu and S Techert, MPI Gottenburg

Light driven [2 +2] cycloadditon of 2-Benzylidene Cyclopentanone

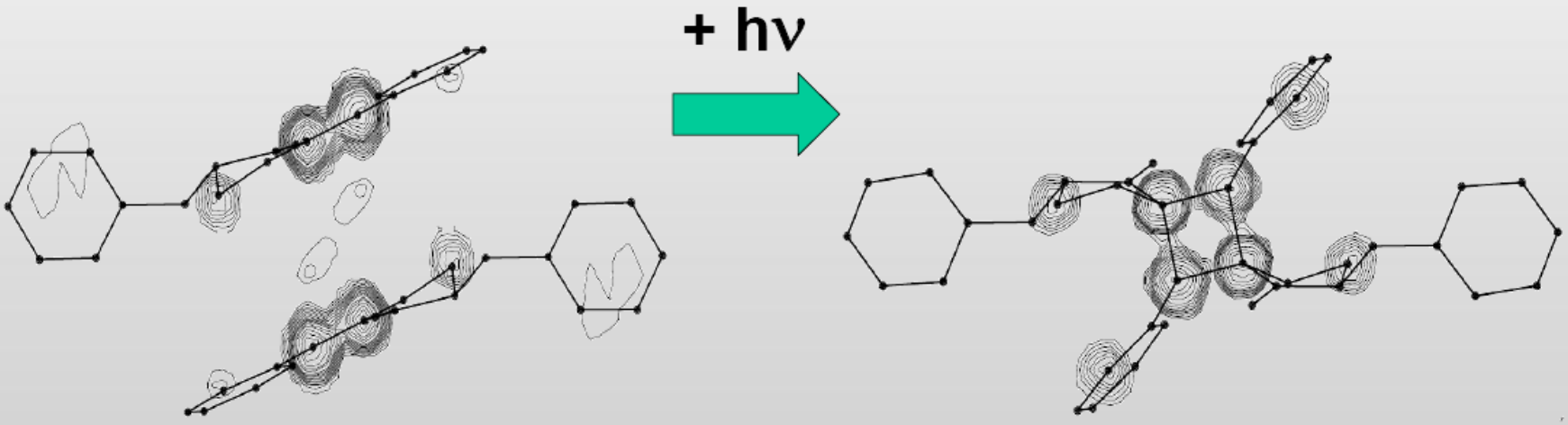

Photochemisty

Work of J Davaasambuu and S Techert, MPI Gottenburg

Light driven [2 +2] cycloadditon of 2-Benzylidene Cyclopentanone

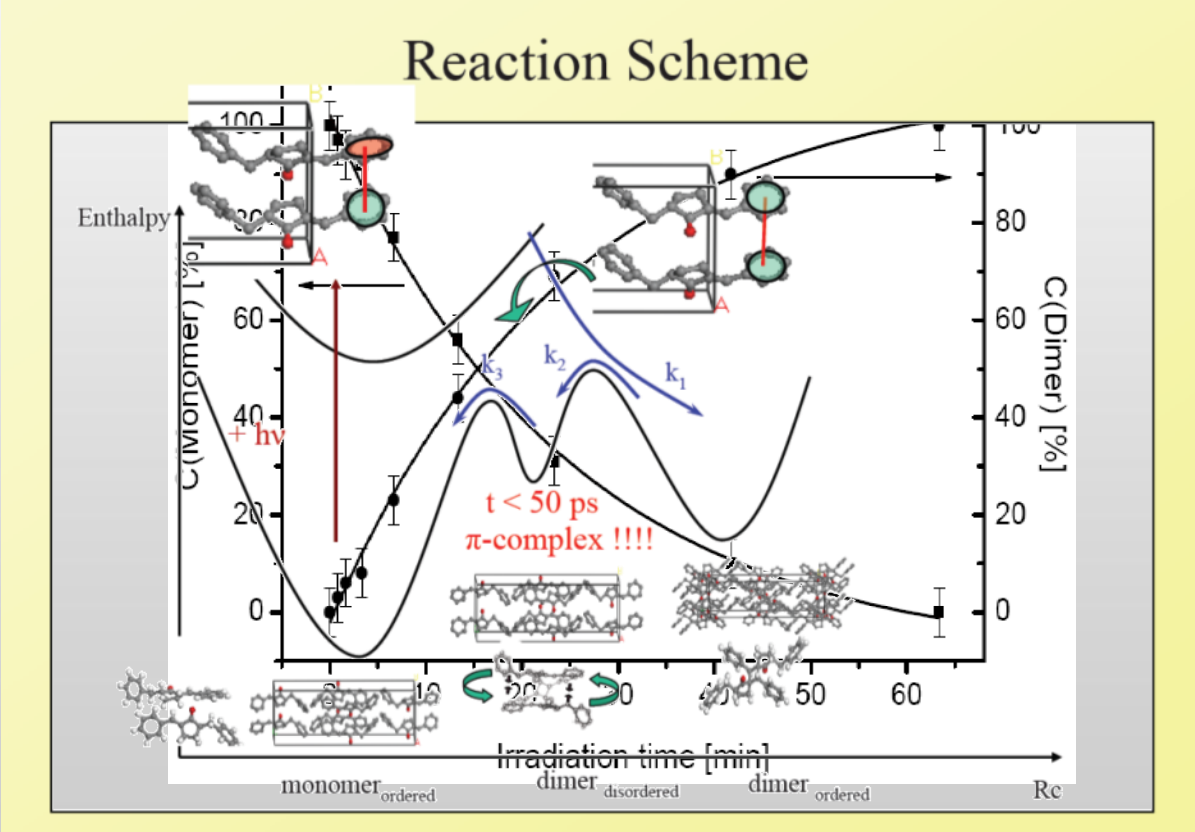

Monomer Refinement

- **Monomer: 12 grains found**

Orthorhombic, Pbca
a=8.59Å, b=10.61Å c=31.10Å

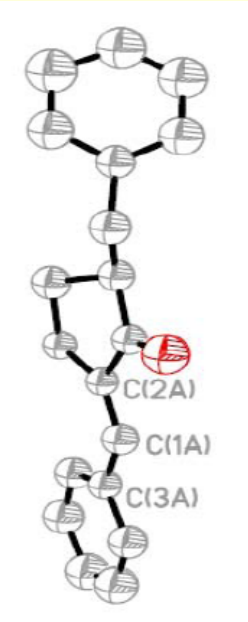

Grain	R(int),%	R(sigma),%	GooF	R1,%
1	6.2	2.8	1.07	5.69
2	6.2	7.5	1.02	5.80
3	5.2	2.6	1.05	4.66
4	7.8	4.1	1.03	6.55
5	5.8	6.8	1.04	6.60

Intermediate Refinement

- **Intermediate Phase: 16 grains found**

Orthorhombic, Pbca
a=8.58Å, b=10.76Å c=30.79Å

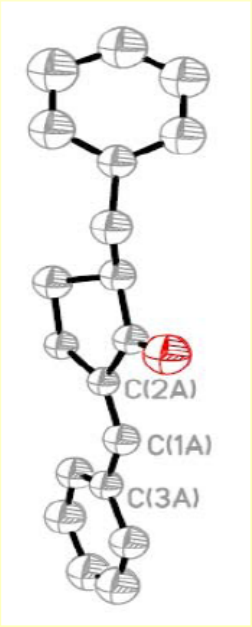

Grain	R(int),%	R(sigma),%	GooF	R1,%
1	11.1	5.2	1.11	15.85
2	10.1	4.6	2.02	16.03
3	13.8	6.2	1.10	12.13
4	10.8	4.1	1.03	15.55
5	11.5	5.4	1.06	15.30

The poor R1 is due to the incompleteness of the reaction

Two Phase Refinement

- **Refinement of Intermediate Phase including Dimer: 16 grains found**

Orthorhombic, Pbca
a=8.58Å, b=10.76Å c=30.79Å

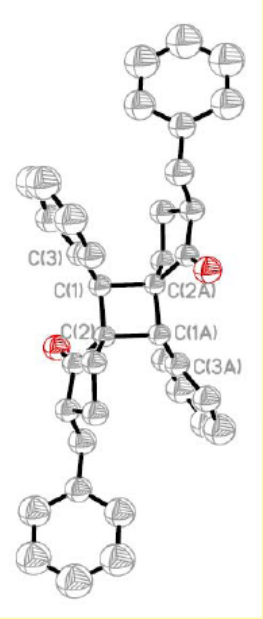

Grain	R(int),%	R(sigma),%	GooF	R1,%
1	9.4	6.3	0.90	6.91
2	6.2	7.5	1.07	7.42
3	7.1	10.5	1.05	6.83
4	9.6	10.7	1.02	6.81
5	6.8	8.8	1.03	6.60
6	8.2	7.4	1.03	6.33
7	6.8	7.2	1.02	6.07
8	7.0	9.2	1.04	6.33
9	6.9	7.2	1.01	5.67
10	7.0	9.3	1.04	6.21

Two phase refinement brings R1 back to 6%!

-single crystal quality fit from polycrystalline data taken during a 1st order transition

Time resolved studies (ID11, ID15, ID31)

5 ms data

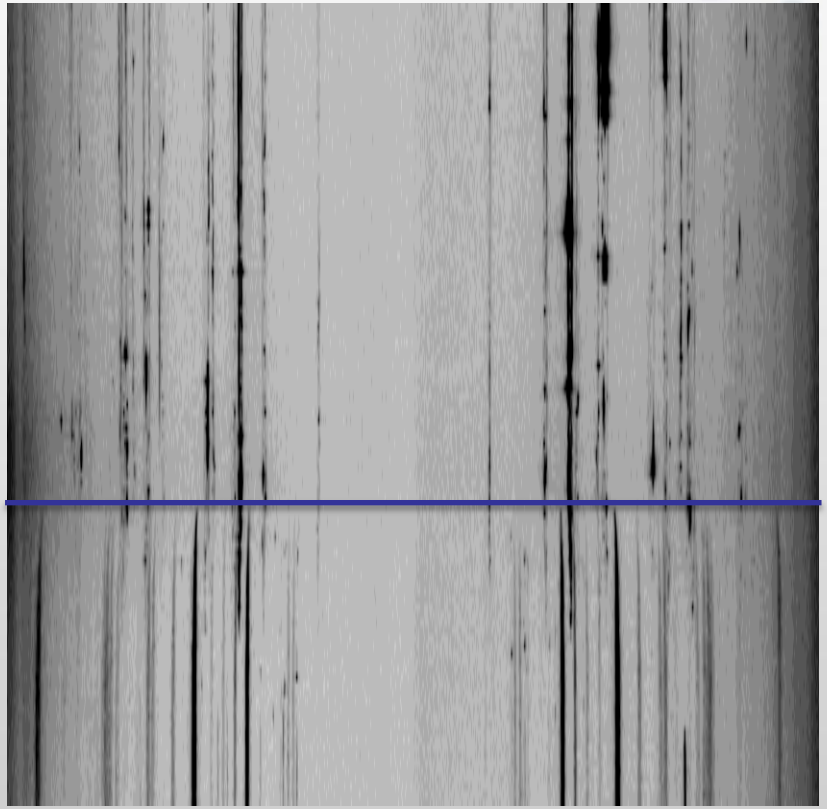

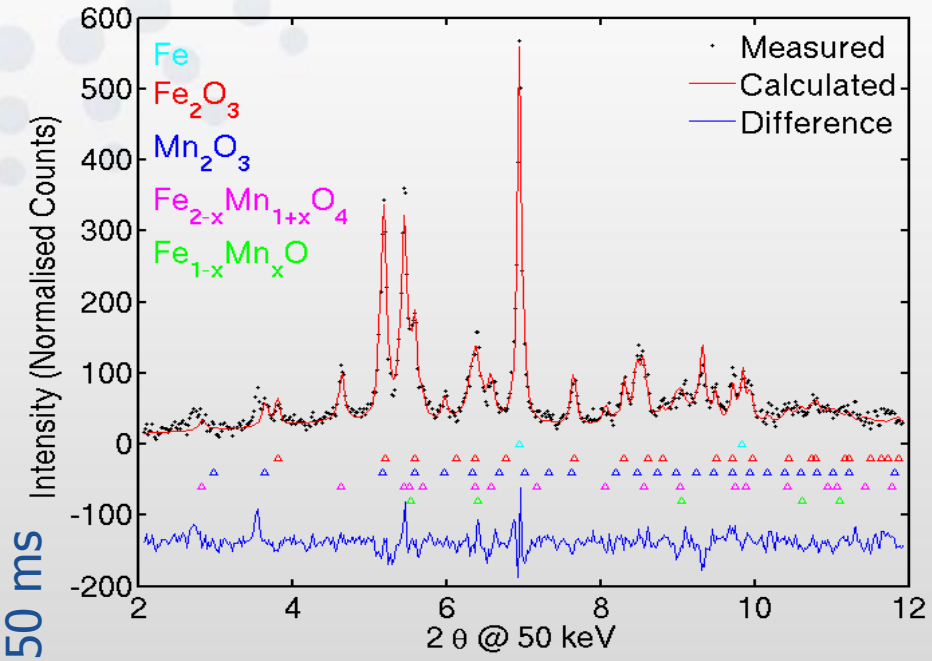

Combined XRD-IR-MS

Three Way Catalysts (ID15)

Diminish polluting emissions from gasoline engine powered vehicles

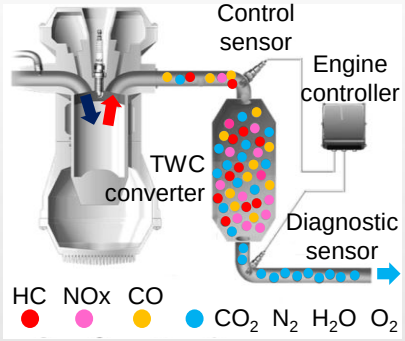

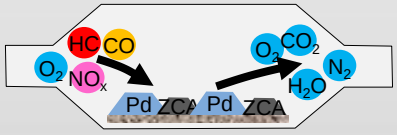

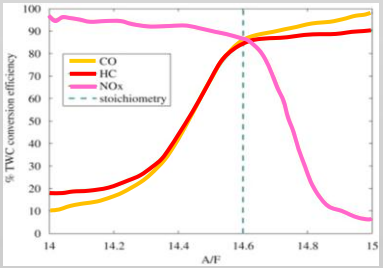

Remove from exhaust gasses
- Carbon Monoxide (CO)
- un-burnt Hydrocarbons (HC)
- Oxides of Nitrogen (NO_x)

TWC converter simultaneous tasks
- Oxidize CO to CO_2
- Oxidize HC to CO_2 and H_2O
- Reduce NOx to N_2

TWCs main components
- Support (Al_2O_3)
- Catalyst (Pd, Pt, Rh nanoparticles)
- Promoter ($CeZrO_4$ nanoparticle)

TWC operation for optimum performances
- engine running with air / fuel = 14.6 – 14.8 (by weight)
- exhaust gas oscillating (1-3Hz) between excess fuel and excess oxygen conditions

More in detail

Oxidation reactions with O_2:

$CO + ½\ O_2 \rightarrow CO_2$
$HC + ½\ O_2 \rightarrow CO_2 + H_2O$
$HC + ½\ O_2 \rightarrow CO + H_2O$
$H_2 + ½\ O_2 \rightarrow H_2O$

Oxidation/reduction reactions with NO:

$CO + NO \rightarrow ½\ N_2 + CO_2$
$HC + NO \rightarrow N_2 + H_2O + CO_2$
$HC + NO \rightarrow N_2 + H_2O + CO$
$H_2 + NO \rightarrow ½\ N_2 + H_2O$
$H_2 + 2\ NO \rightarrow N_2O + H_2O$
$5/2\ H_2 + NO \rightarrow NH_3 + H_2O$
$2\ NO + 2\ NH_3 + ½\ O_2 \rightarrow 2N_2 + 3\ H_2O$

Water–gas shift reaction:

$CO + H_2O \rightarrow CO_2 + H_2$

Reforming reactions:

$HC + H_2O \rightarrow CO_2 + H_2$
$HC + H_2O \rightarrow CO + H_2$

Combined XRD-IR-MS

Role of Pd nanoparticles in CO dissociation?

From literature

$2CO + O_2 + Pd \rightarrow 2CO_2 + Pd$

$2NO + 2CO + Pd \rightarrow N2 + 2CO2 + Pd$

No CO dissociation on Pd

4%wt Pd / Al2O3 catalysts during CO/NO cycles (period 27.7 s) at 673ºK

MS

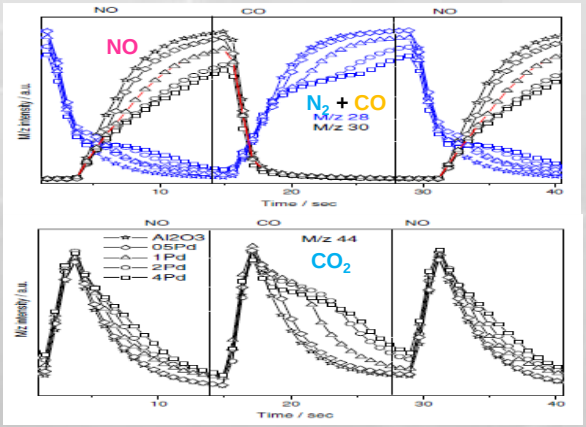

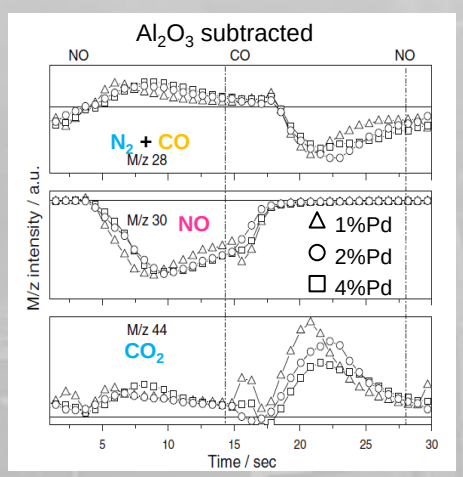

DRIFTS

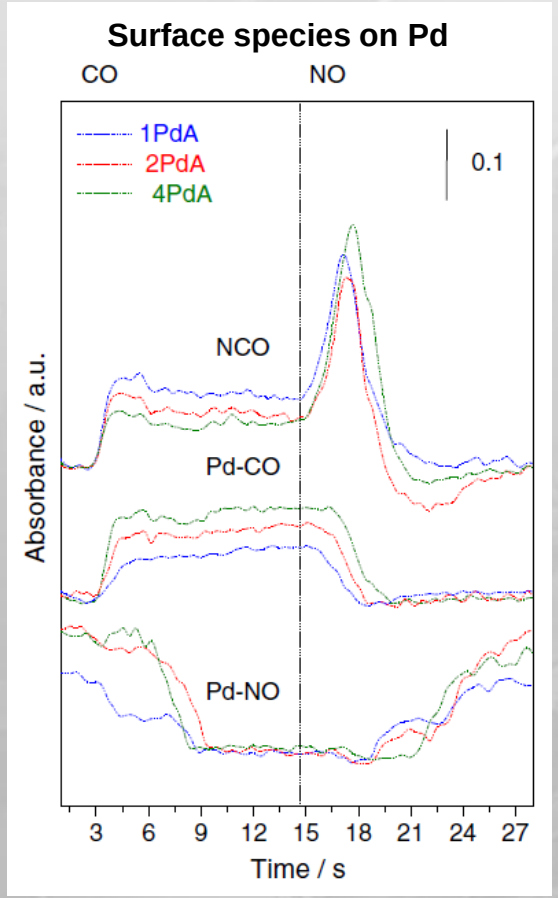

XRD

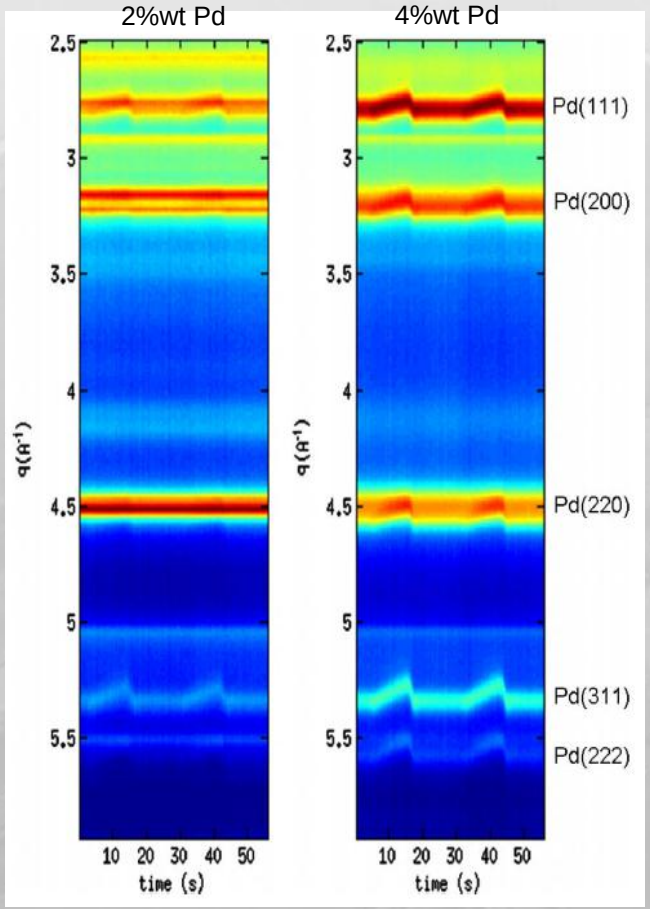

Combined XRD-IR-MS

Summary

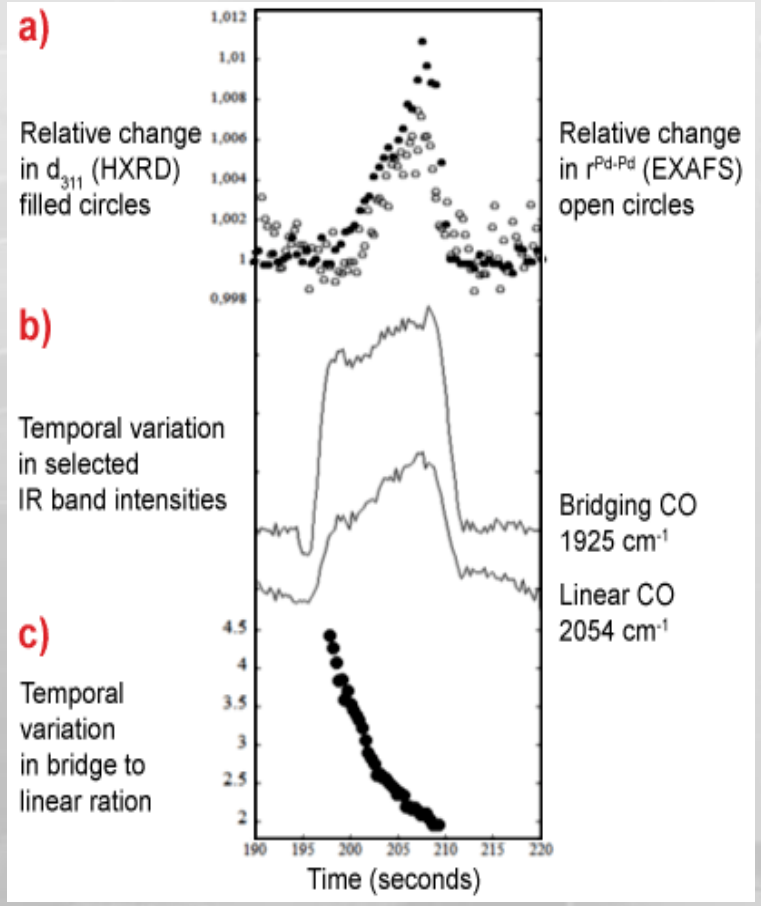

Contrary to what believed
CO dissociates on Pd

C diffusion into Pd lattice → PdC_x

under NO, PdC_x disappears quickly to form NCO

CO linear to bridge ratio changes indicating a size/shape change probably due to C storage

M. A. Newton et al., J. Am. Chem. Soc. ***132****, 4540 (2010)*
A. Kubacka et al., J. Catal. ***270****, 275 (2010)*

Combined XRD-IR-MS

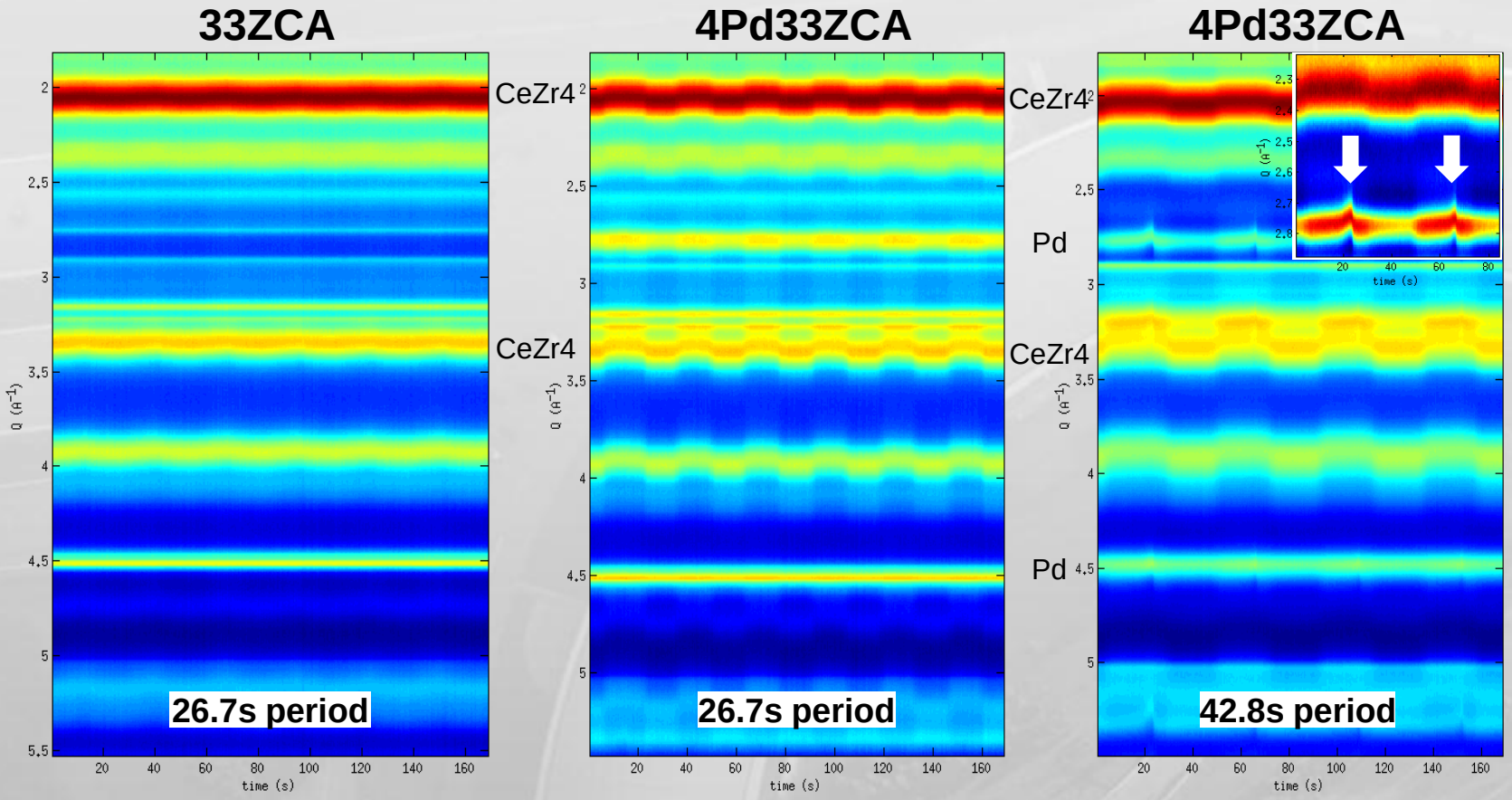

SHORT PERIOD

Pd lattice parameter does not change

$CeZrO_4$ lattice parameter does change

LONG PERIOD

towards the end of CO phase Pd changes as if $CeZrO_4$ were not present

Conclusions

Combining XRD-IR-MS new interplay
between Pd and $CeZrO_4$ have been discovered:

1. Inhibition of formation of PdC_x phases during CO cycle through Oxygen release

CO dissociation is still occurring (formation of Pd(CN))
BUT
$CeZrO_x$ provides Oxygen to the adsorbed C atoms to efficiently produce CO_2

2. Enhanced reducibility of nano-$CeZrO_4$ phase when in contact with Pd

contact with Pd nanoparticle promotes CeZrO4 oxygen transfer

3. Increased structural stability during redox cycles

Pd nanoparticles do not change shape

Newton et al., Angew. Chem. Int. Ed. ***51****, (2012) 2363-2367*

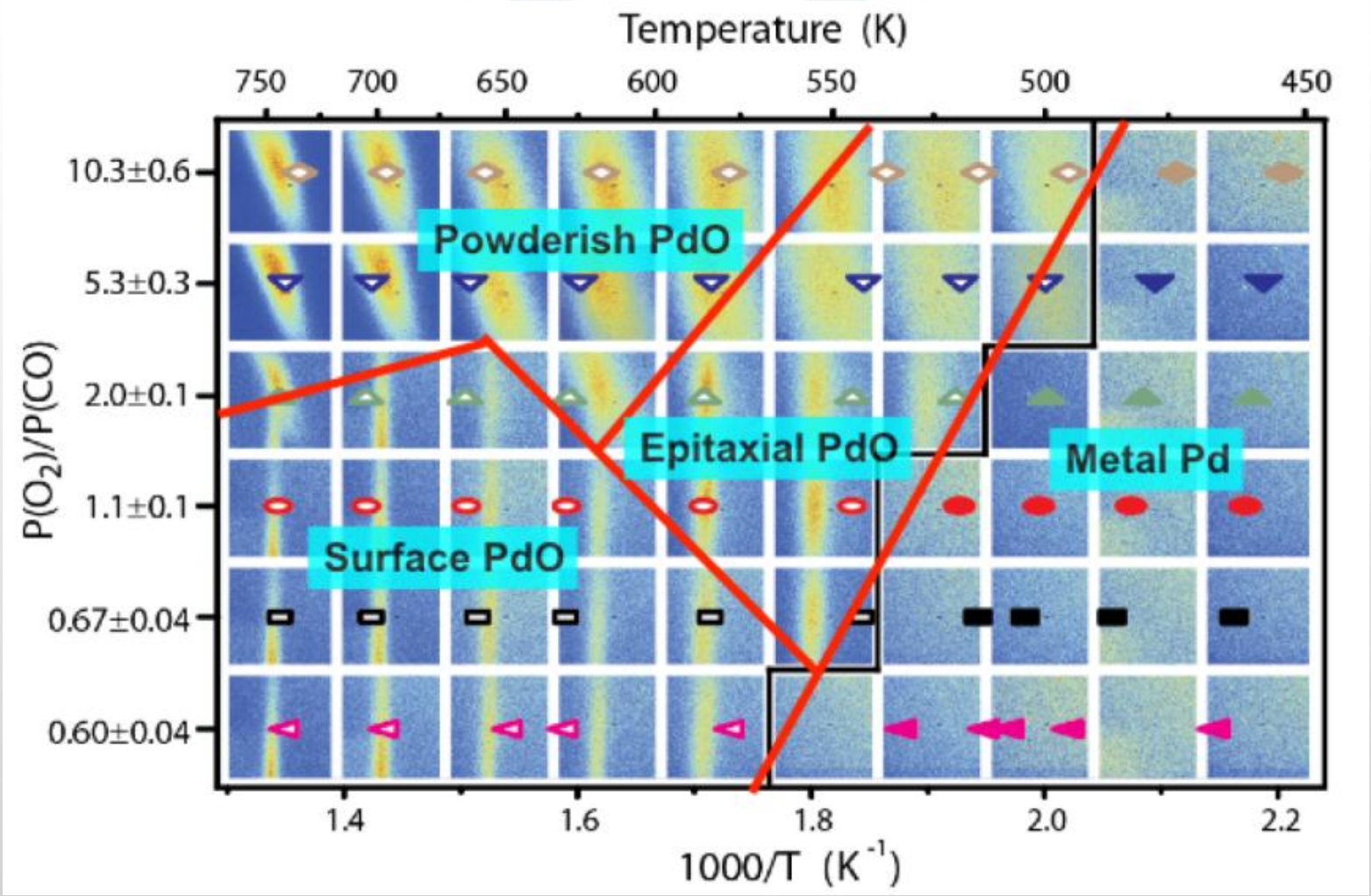

Phase diagram of Pd surface during CO oxidation for different CO/O_2 pressure ratios. R. van Rijn *et al.*, PCCP, in press. *(ID03)*

In-situ characterisation of bainite growth (ID31)

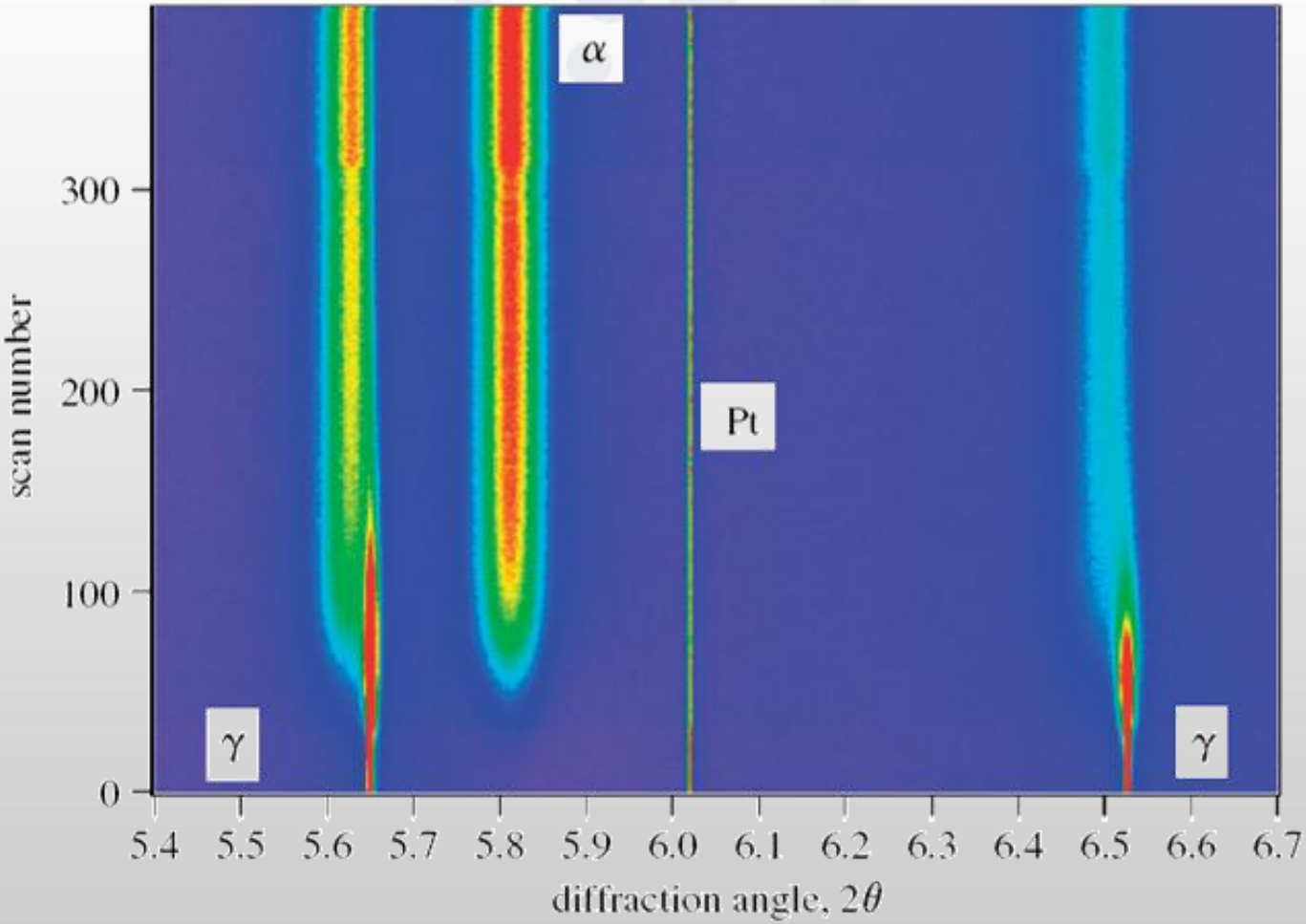

Stone et al., Proc. R. Soc. A, 464, 1009, (2008)

In-situ characterisation of bainite growth [60 keV]

Evolution of diffraction peaks γ{111} and α{110}

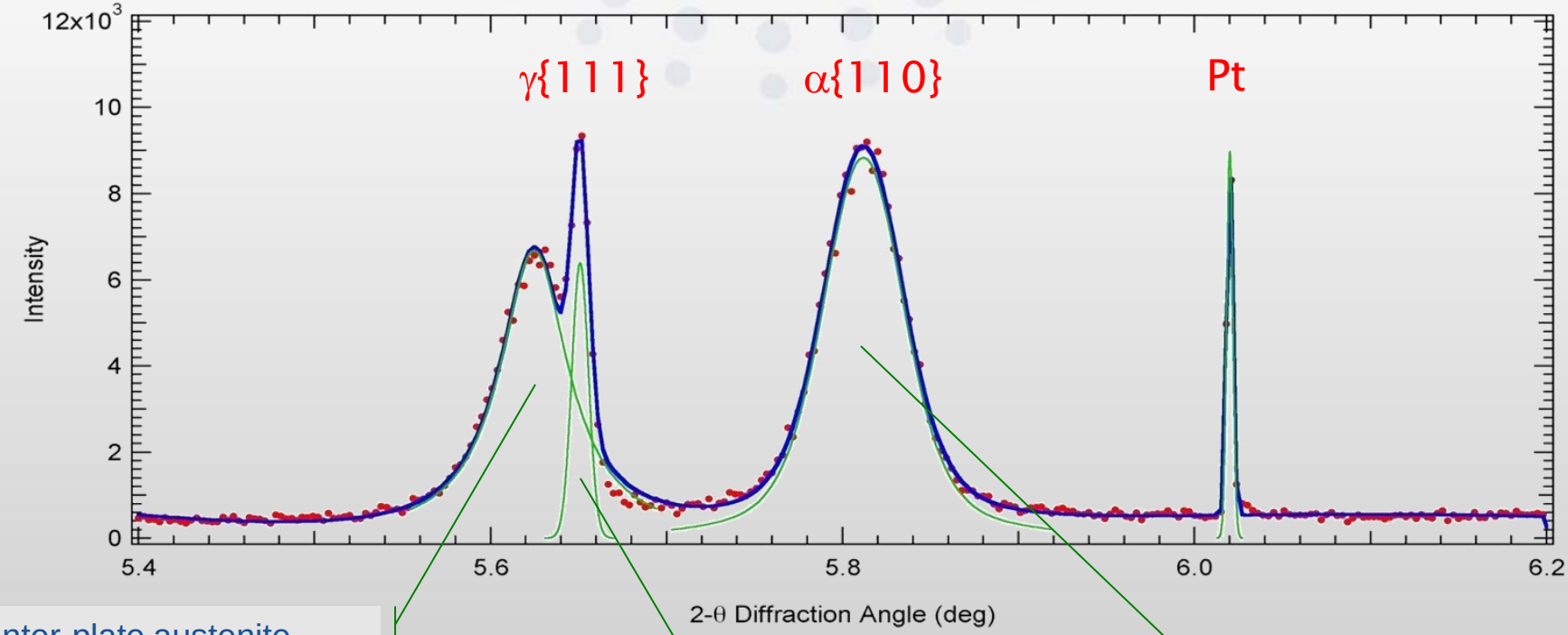

Inter-plate austenite carbon-rich, larger lattice parameter, lower 2θ, broadened peak (small grains / large strains)

Original austenite bulk carbon content sharp peak (large grains / low strains)

Bainitic ferrite broadened peak (small grains / large strains)

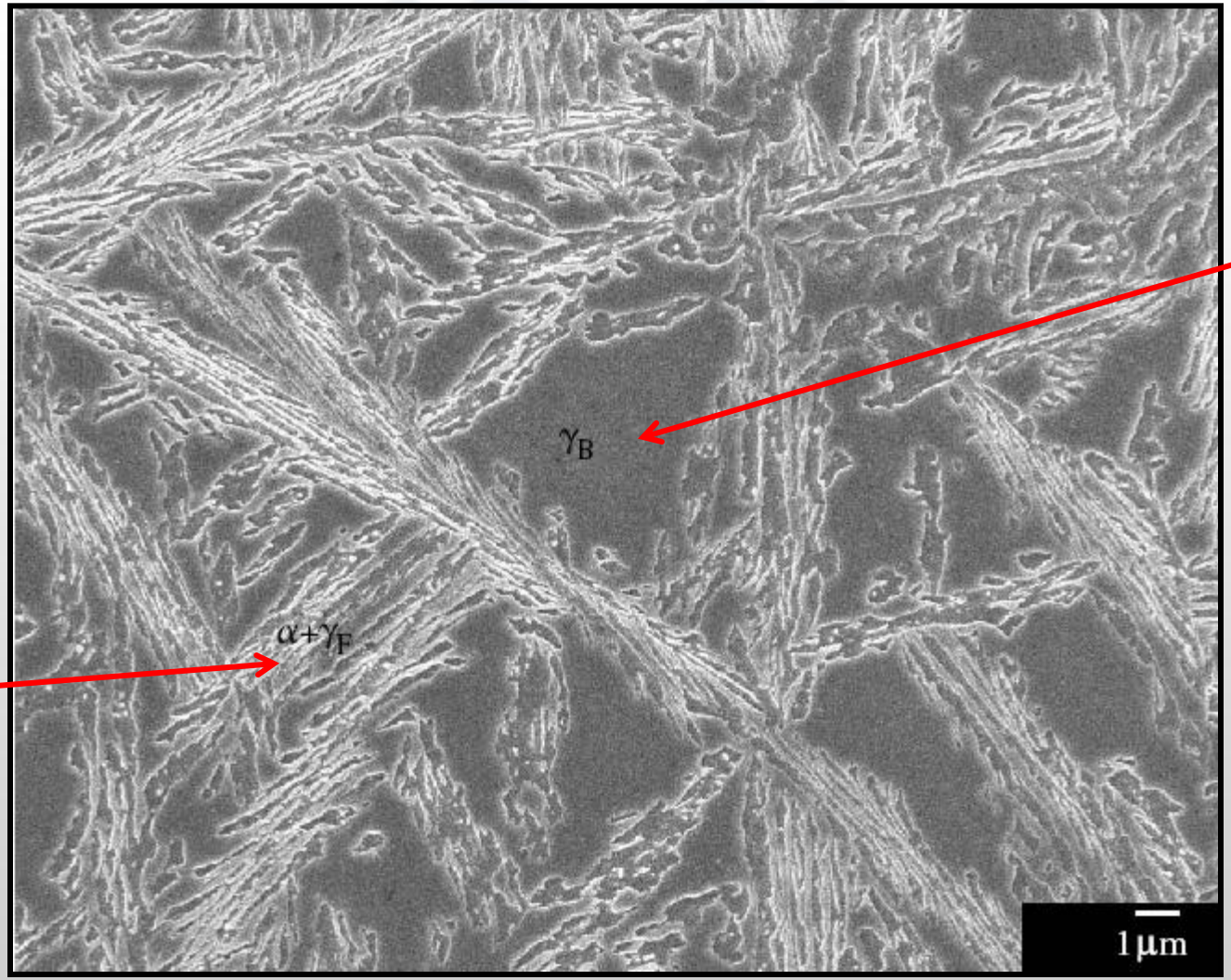
Residual austenite
Bainitic ferrite and films of austenite
γ_B
$\alpha+\gamma_F$
1 µm

Spatial Resolution

Resolution is tied to

- Beam size
- Detector Resolution
- Stability
- Reconstruction algorithms; use of additional information

- For 2 dimensional direct (transmission or reflection) mapping, the resolution is ultimately equivalent to the beam size.
- Beam size depends on the focusing optics and the source
  - Upgrade -> much improved source will give a huge improvement in focusing capability

Diffraction Mapping – Direct Mapping in 2d

- Powder Diffraction
- Spatial resolution determined by
  - Beam size
  - Accuracy of translations
  - Metrology of beam
  - = O(100 nm)
- Multi-dimensional Map
  - Phases
  - Strain
  - Stoichiometry
  - Microstructure
  - …

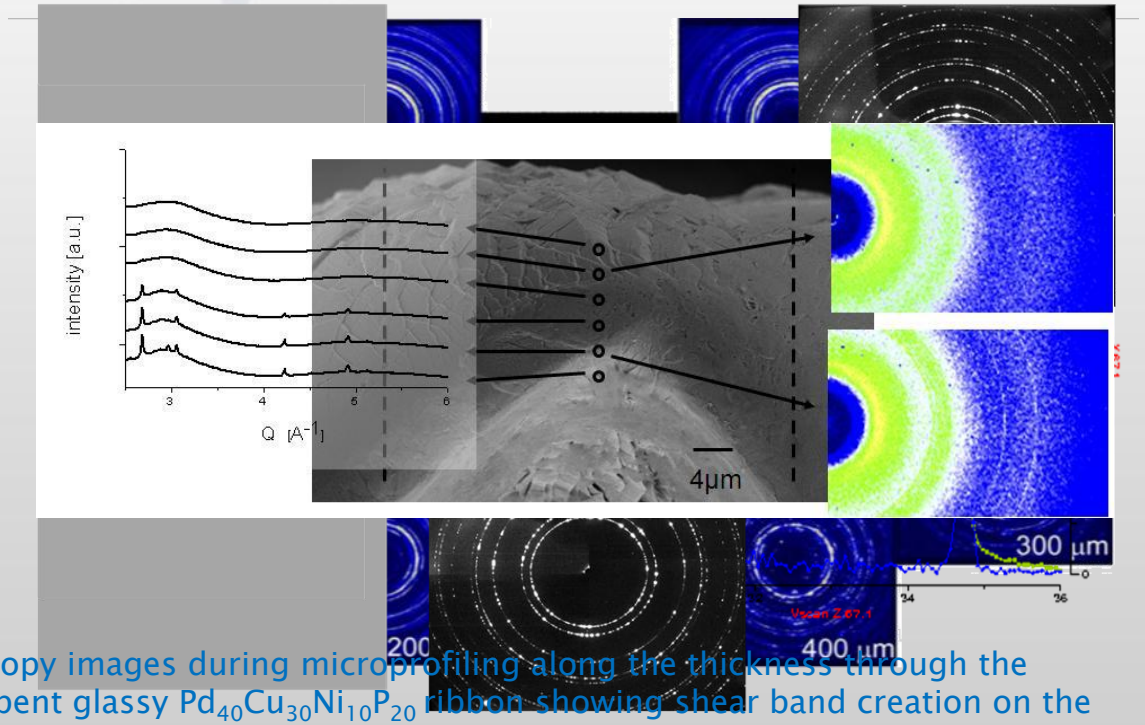

X-ray microscopy images during microprofiling along the thickness through the width of bent glassy $Pd_{40}Cu_{30}Ni_{10}P_{20}$ ribbon showing shear band creation on the compression side only.

Yavari et al., PRL 2012
Yavari et al., Scripta Metall. 2008
Gerbert et al., in preparation

Scanning Diffraction Microscopy (ID01)

Region of interest:

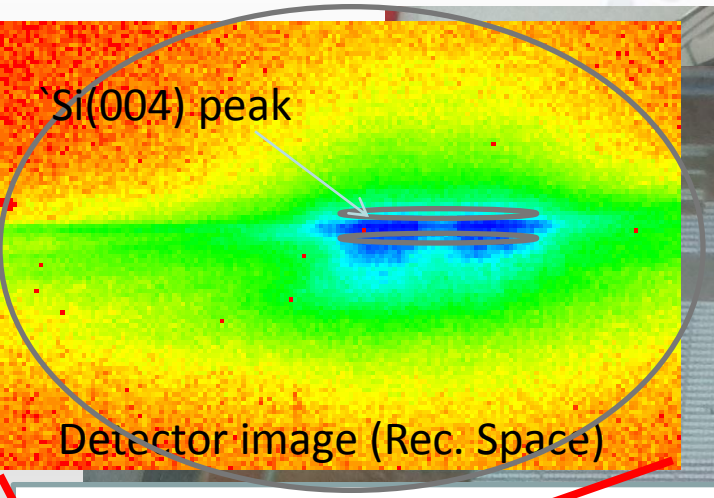

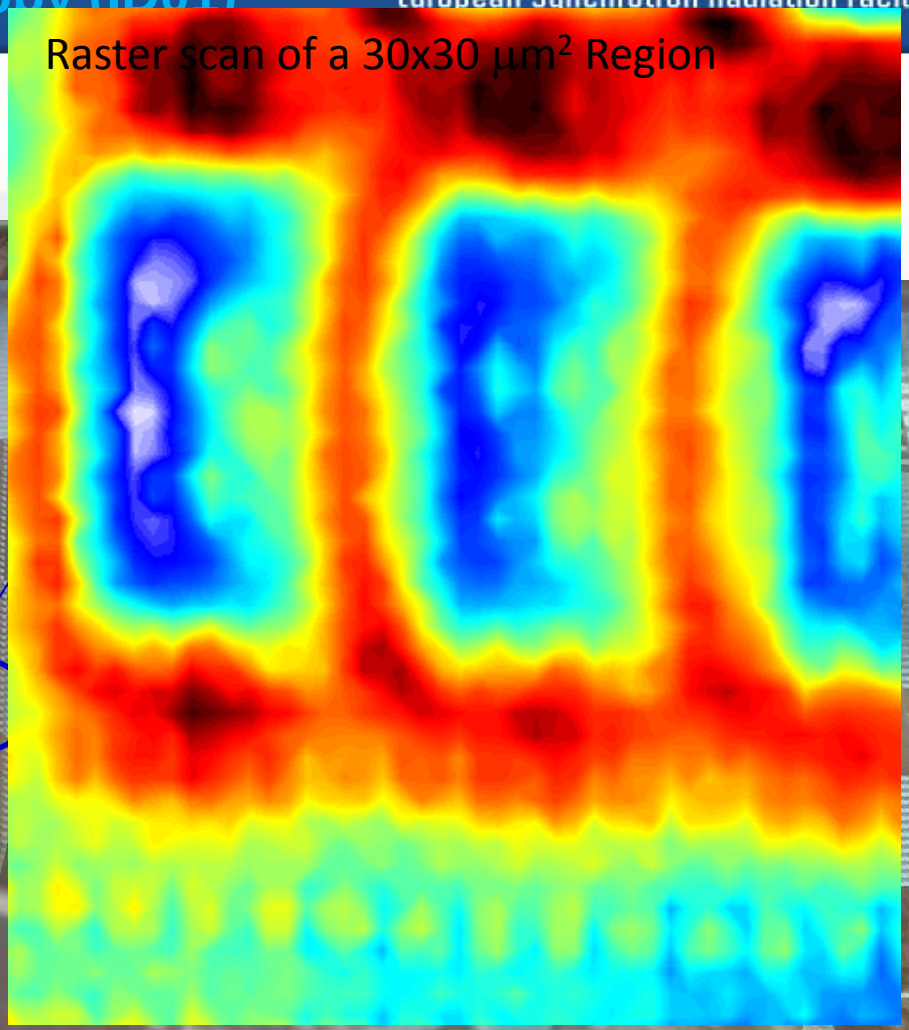

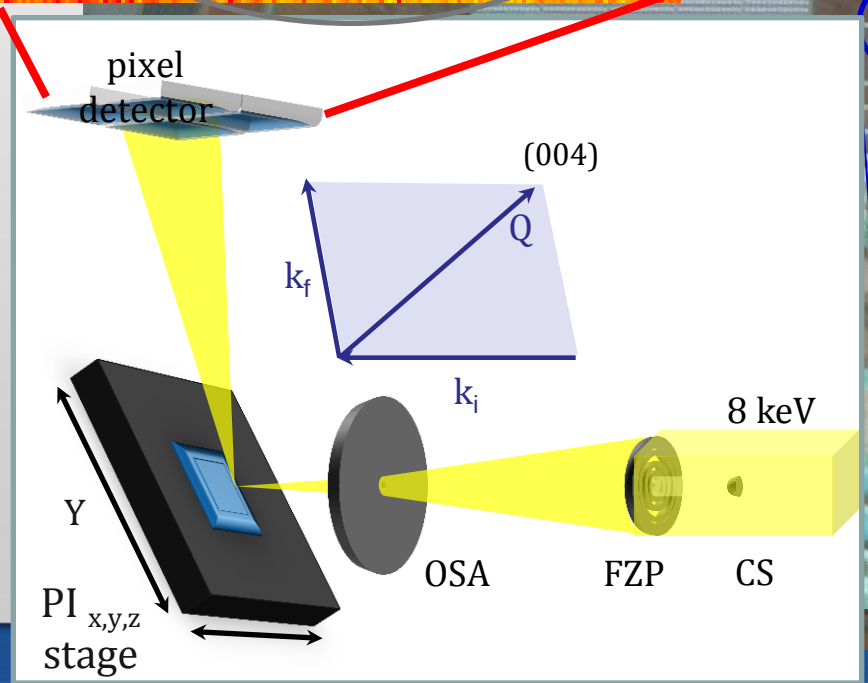

Lens-less microscopy (ID01)

…refers to the use of diffraction of coherent x-rays *&* mathematical algorithms – rather than lenses, to *retrieve* the image of the sample with *nm resolution* in a model-free way

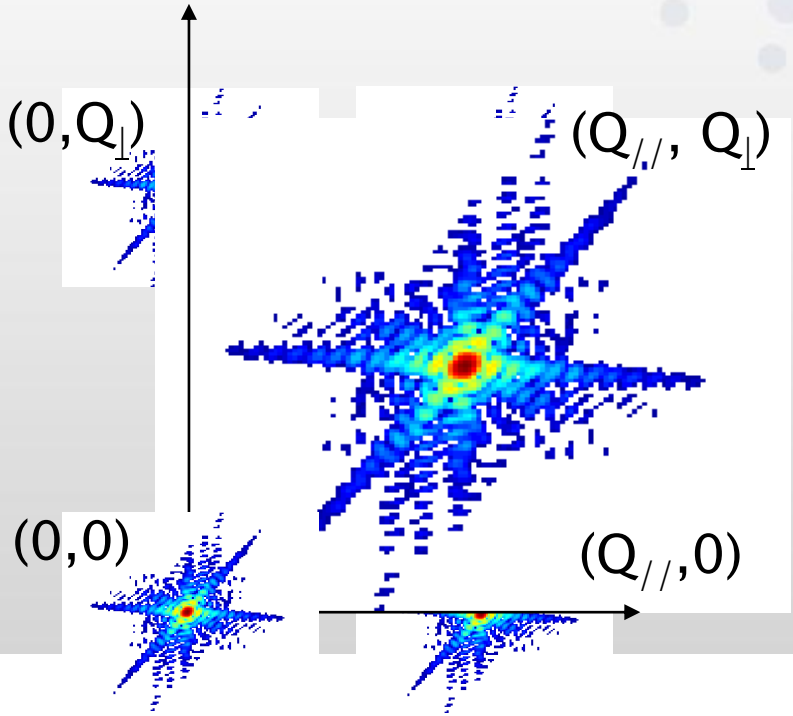

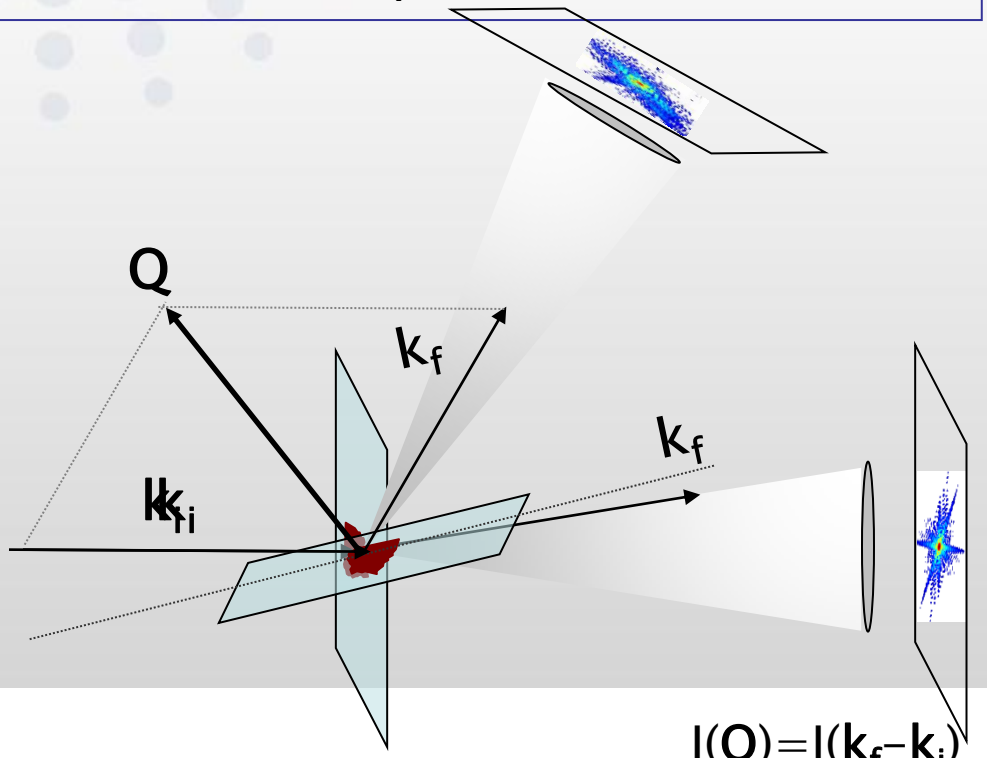

Object shape

Crystal structure

$I(\mathbf{Q}) = I(\mathbf{k_f} - \mathbf{k_i})$

$I_i = I_f$

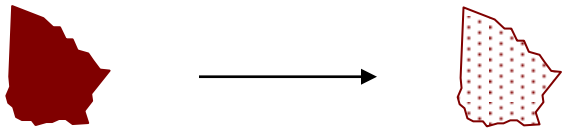

Surface Diffraction (ID03)

In-situ studies of the structure and morphology of surfaces either under static conditions (surface crystallography) or in situ during surface processes (heterogeneous catalysis, surface reactions, growth, ...)

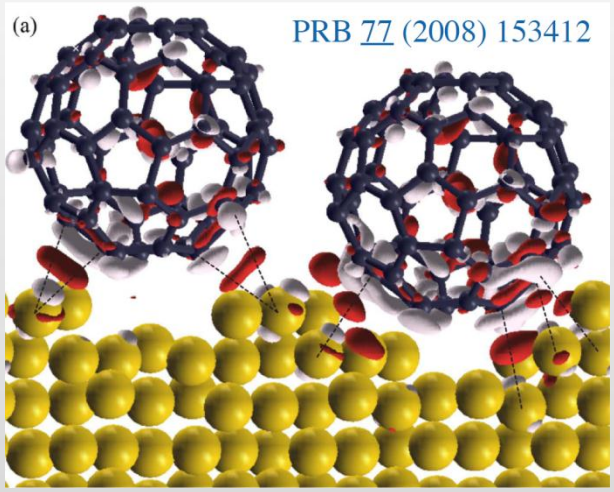

Techniques:
- Surface X-ray diffraction
- Grazing incidence small angle scattering
- X-ray reflectivity
- Anomalous diffraction (including DAFS)
- Coherent diffraction

Optics:
- Energy range 5-28 keV
- Typical focal size 20x20 μm^2 with 10^{13} ph/s
- Min focal size 3x3 μm^2 with 10^{12} ph/s

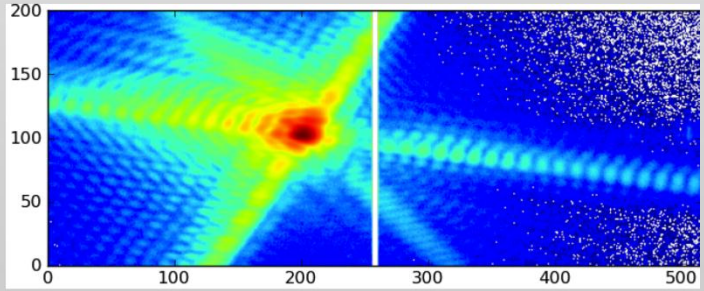

Coherent diffraction from a gold nanorod

UHV surface scattering (ID03)

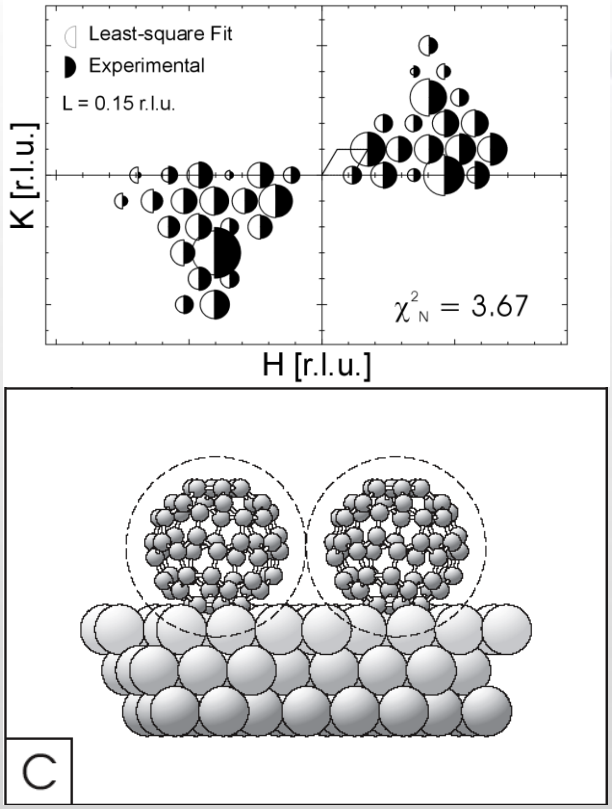

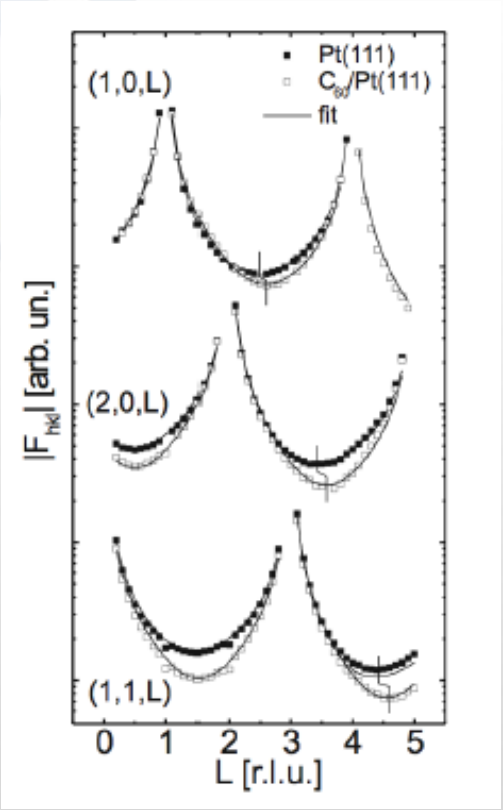

Structural determination of the adsorption of organic molecules on metal surfaces. The case of C_{60} on the Pt(111) surface and the role of surface vacancies.

R. Felici et al., Nature Materials, 4 (2005) 688

HIGH ENERGY MICRO-DIFFRACTION (ID15)

Studies of buried interfaces and liquid surfaces/interfaces

Optics for liquid-liquid interface studies
Si(111)/Si(311) crystals

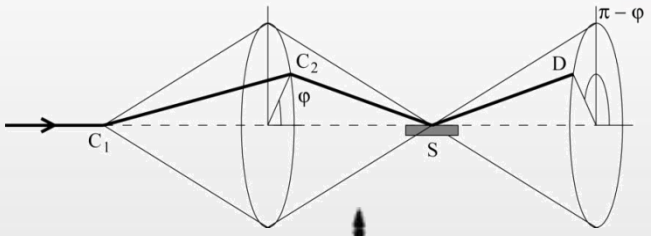

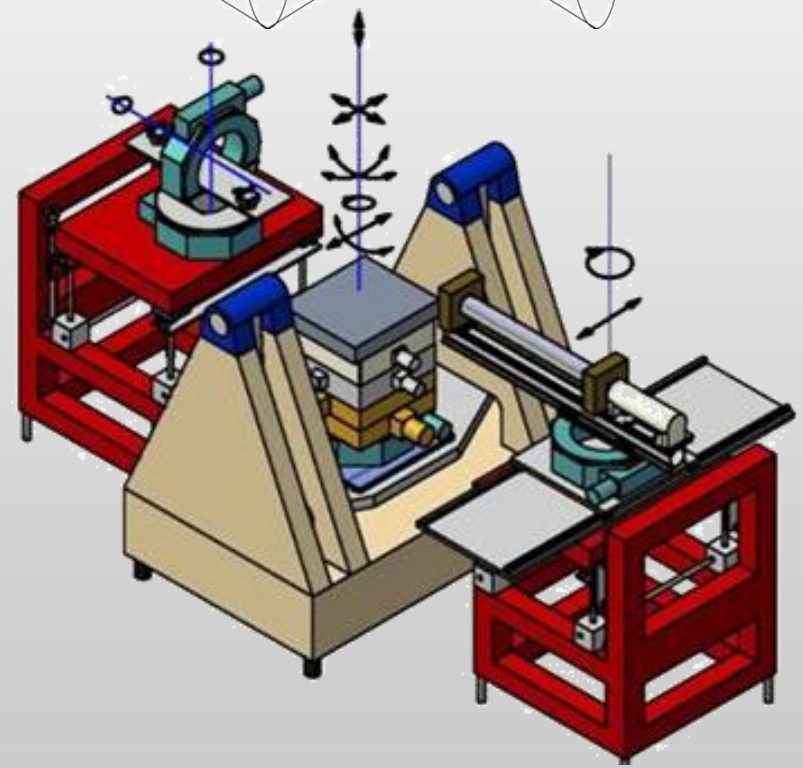

GIANT METAL COMPRESSION AT LIQUID SOLID (Pb-Si, In-Si) SCHOTTKY JUNCTION

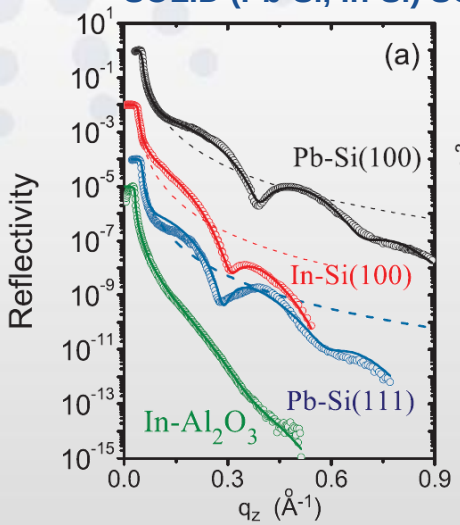

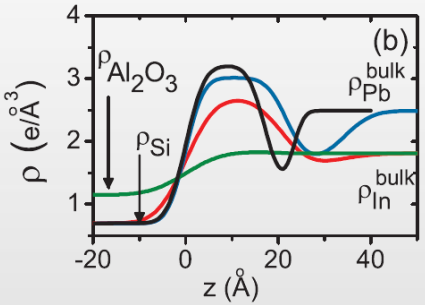

SELF ASSEMBLY OF Au NANOPARTICLES

3nm DT-Au amorphous film

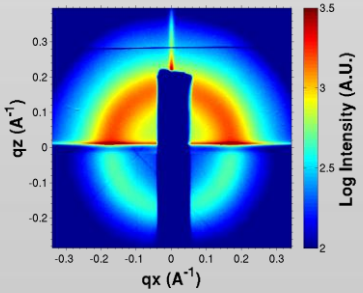

5nm DT-Au ordered monolayer

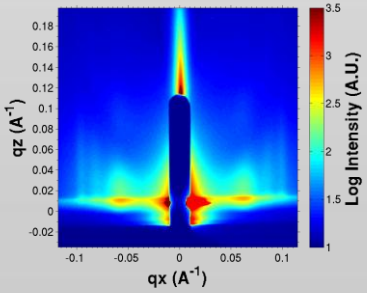

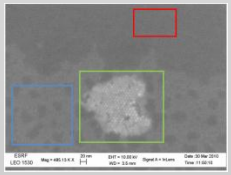

3d reconstruction methods

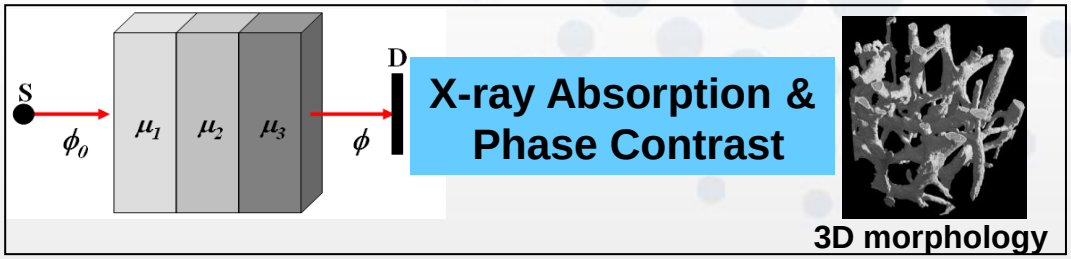

X-ray Absorption & Phase Contrast

3D morphology

Z contrast 0.1 µm

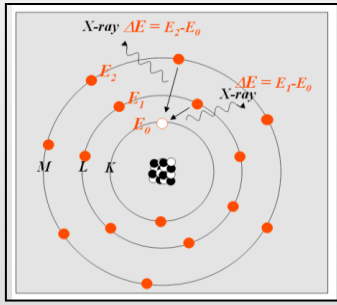

Golosio et al, APL

X-ray Fluorescence

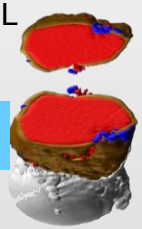

3D chemistry

Elemental contrast 0.1 µm

Structural phase Or crystal Contrast 3-5 µm

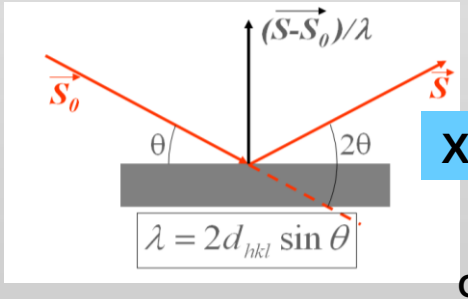

X-ray Diffraction

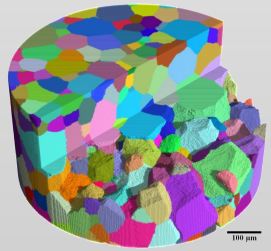

3D crystal phases Or grain distributions

Courtesy of P. Bleuet

*P. Bleuet et al., Nature Materials **7**, 468 - 472 (2008)*

Fast Tomography

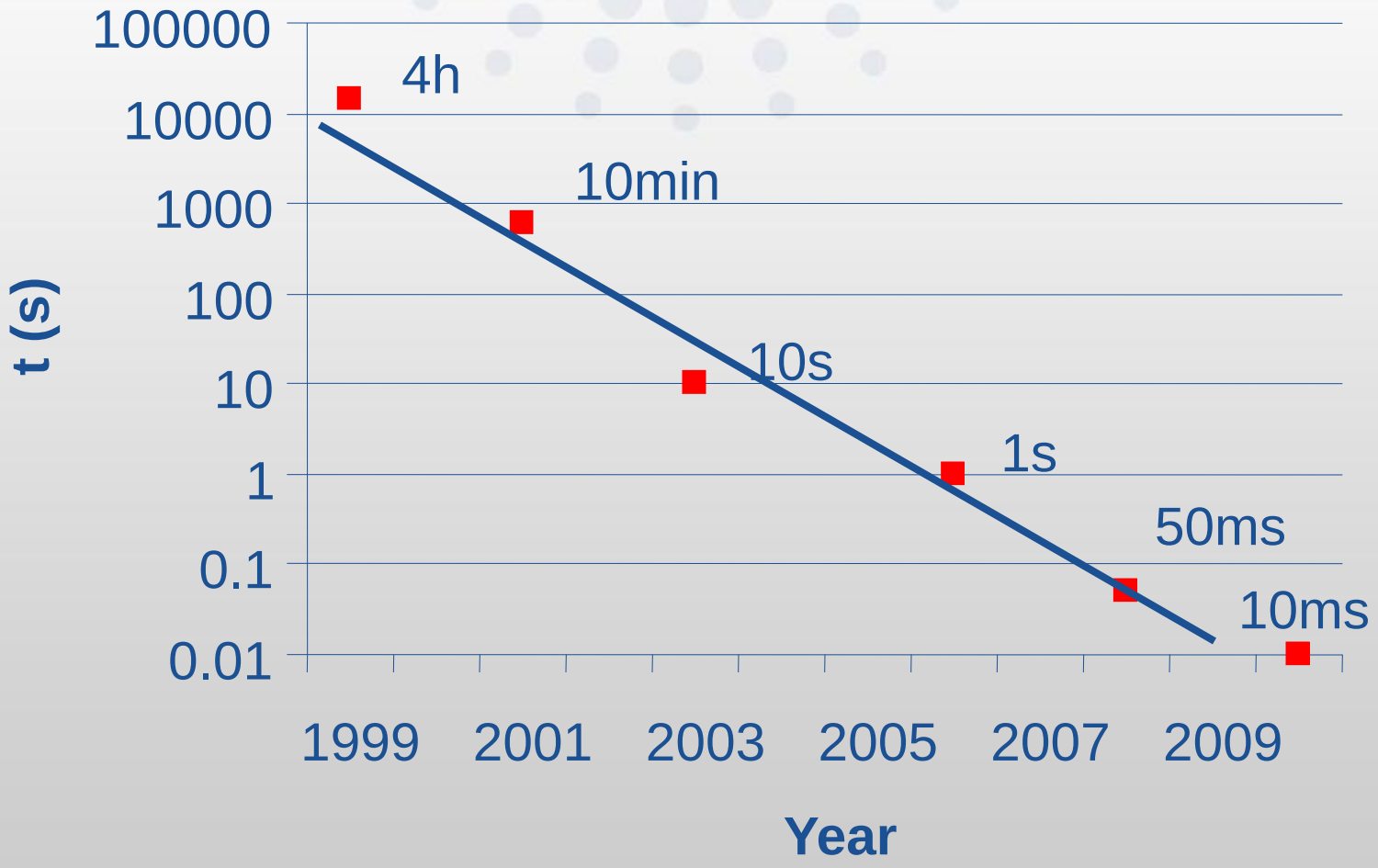

ON THE FORMATION OF VOIDS IN Nb_3Sn "INTERNAL TIN" SUPERCONDUCTING WIRES (ID15)

C. Scheuerlein, M. Di Michiel, A. Haibel

***Appl. Phys. Lett.* 90 (2007)**

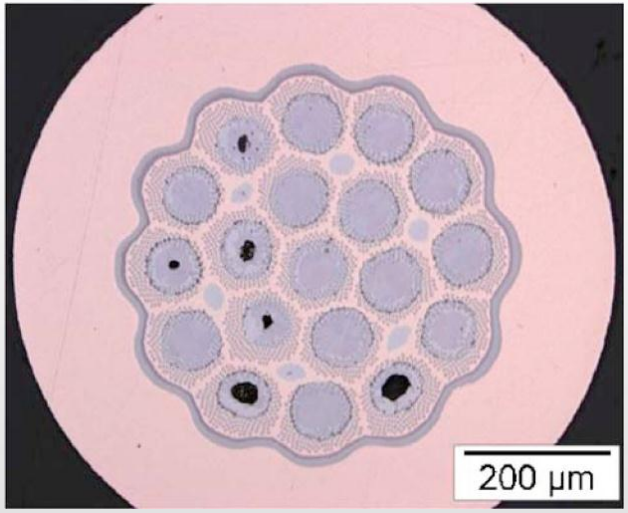

Destructive metallographic techniques: erratic and misleading due to irregularities of strands

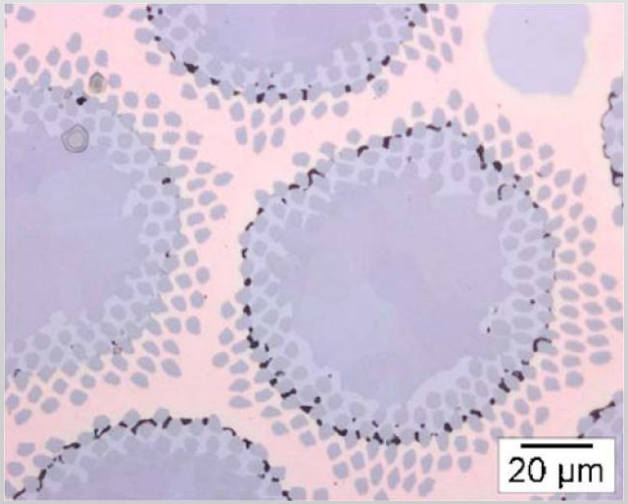

In-situ combined diffraction and tomography study

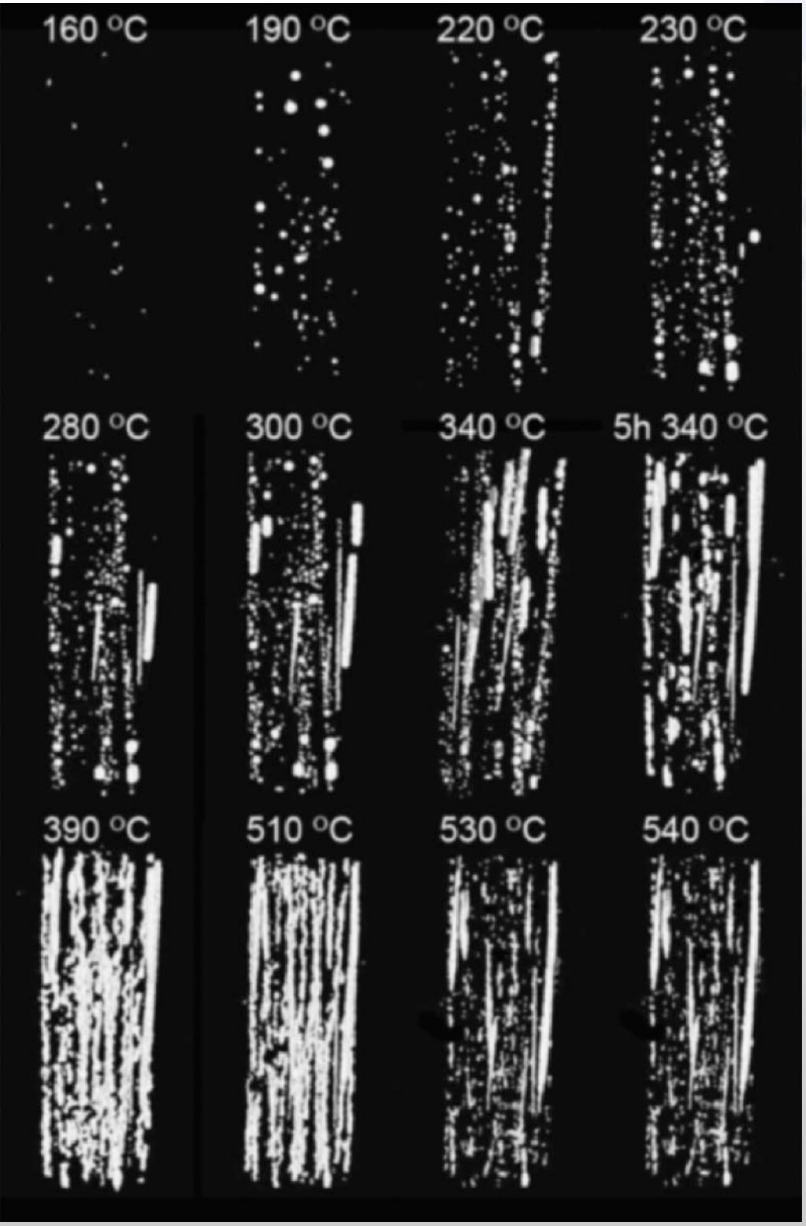

Elongation of voids at 280°C

Agglomeration of globular voids during isothermal step at 340°C

Strong increase of small interfilament voids during isothermal step at 540°C

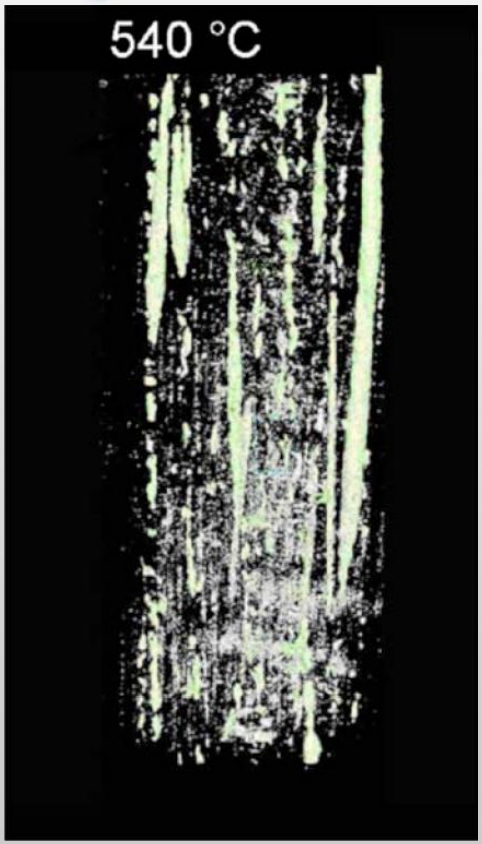

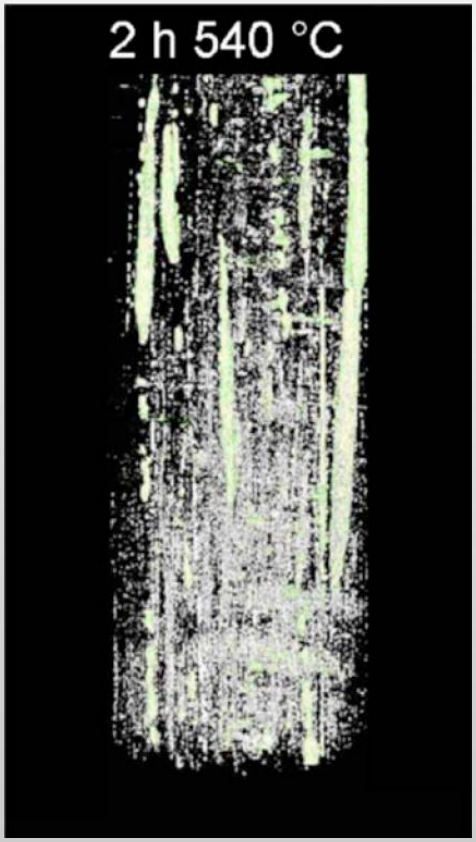

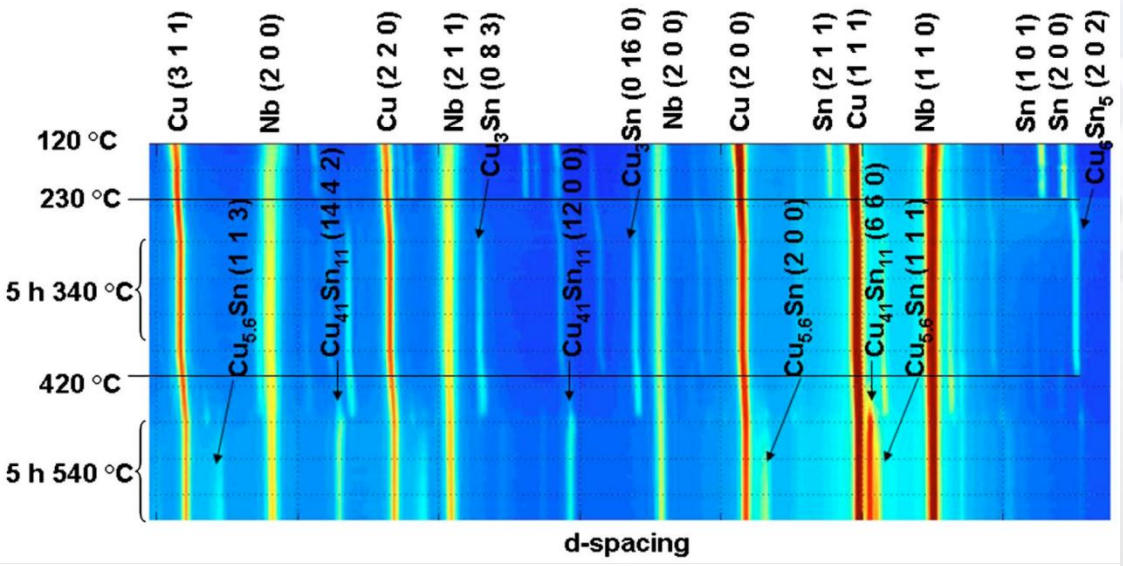

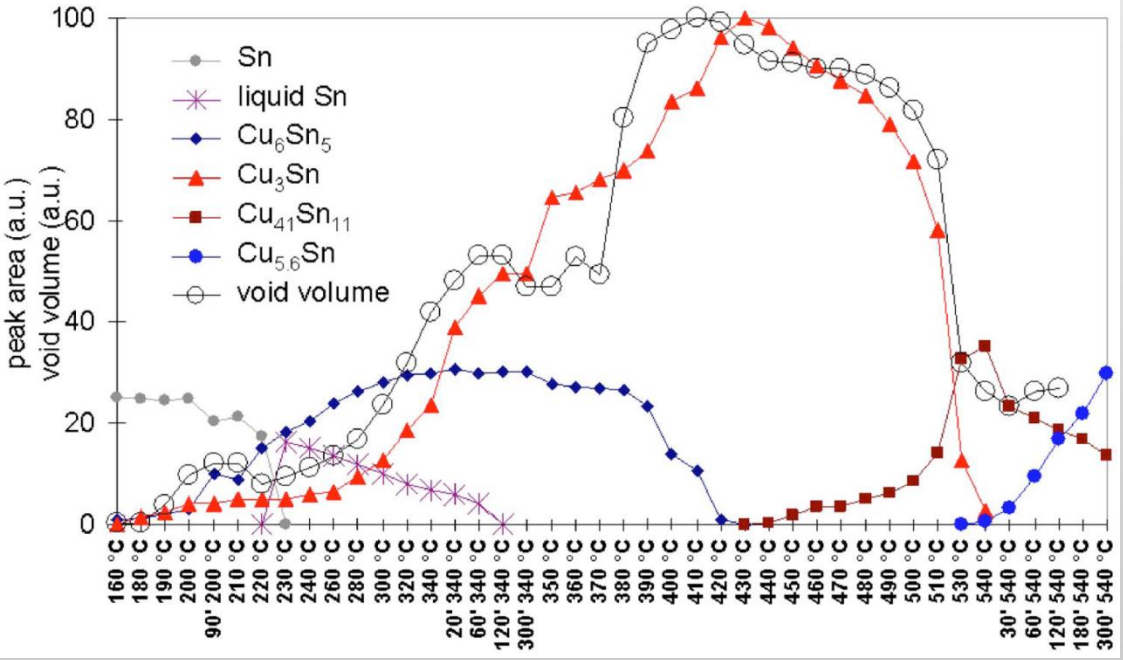

- Agglomeration of voids up to 200°C
- Void growth through density changes; strong correlation with Cu_3Sn content
- Strong increase of small interfilament voids during isothermal step at 540°C but no phase transitions
- **Isothermal holding steps at 340 and 540°C are counterproductive**

XRD-CT (ID15, ID22)

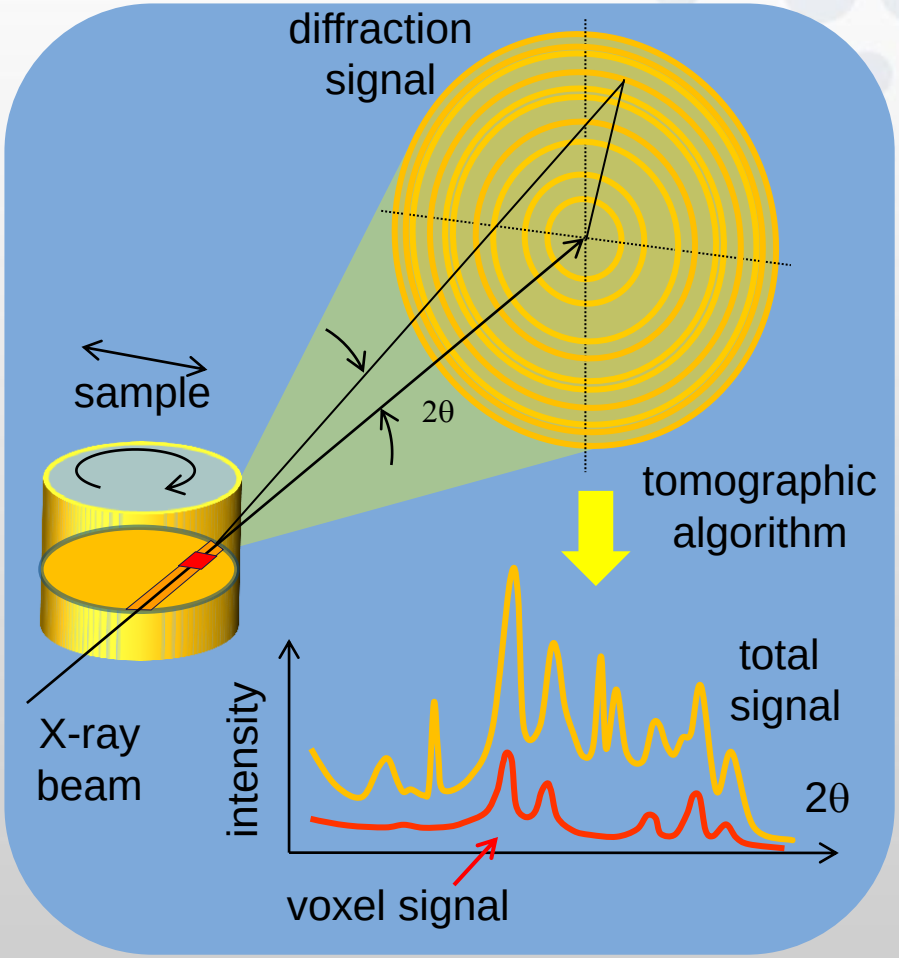

- Spatial resolution is defined by the X-ray beam size Δy
- Temporal resolution depends on
  - sample size / Δy = N
  - detector exposure time 1/f
- Acquisition time per slice
  - ~ N x N / f

  easily many hours if N big!
- XRD-CT was not applied to dynamical samples until 2010
- first experiment on phase evolution during catalyst body preparation

Diffraction Tomography

Phase transformations during processing of superconducting composites

by C. Scheuerlein (CERN), S. Jacques (Manchester), A. Beal (Utrecht), and M. Di Michiel (ID15)

XRD

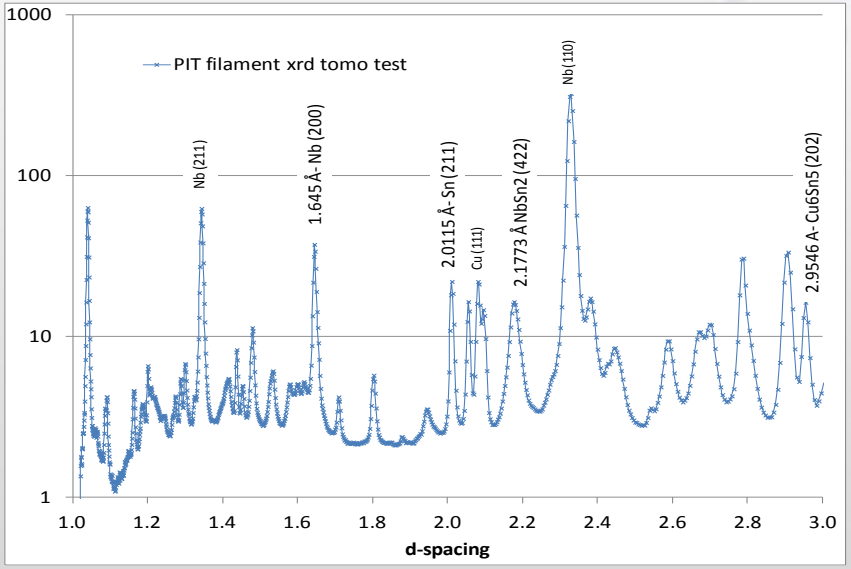

XRD-CT

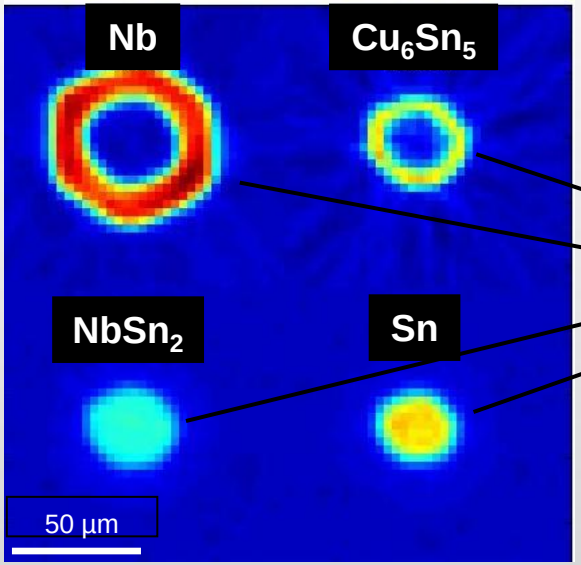

microscope

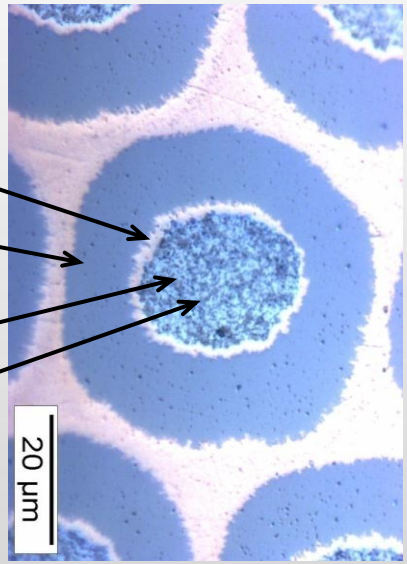

High resolution XRD-CT scans performed in short time

An application where XRD-CT replaces standard absorption and phase tomography

Diffraction Tomography

Phase transformations during processing of superconducting composites

by C. Scheuerlein (CERN), S. Jacques (Manchester), A. Beal (Utrecht), and M. Di Michiel (ID15)

XRD

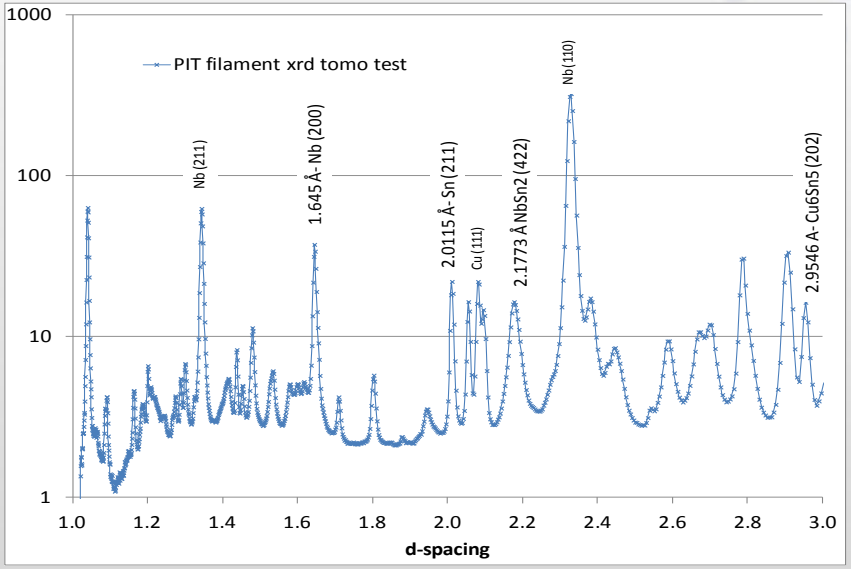

XRD-CT

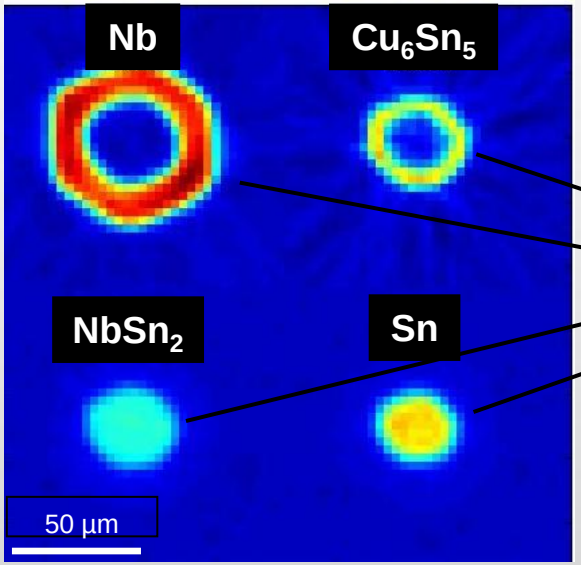

microscope

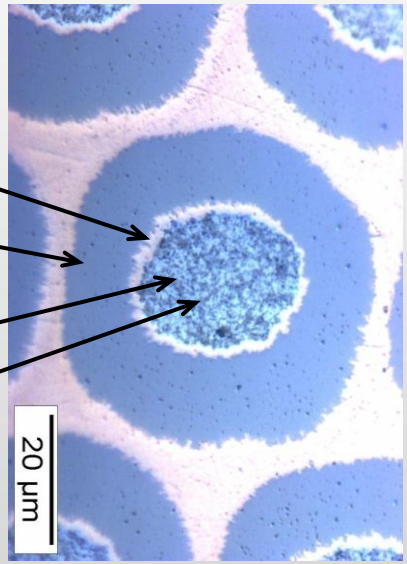

High resolution XRD-CT scans performed in short time

An application where XRD-CT replaces standard absorption and phase tomography

100 years later...

Friedrich and Knipping (Laue)

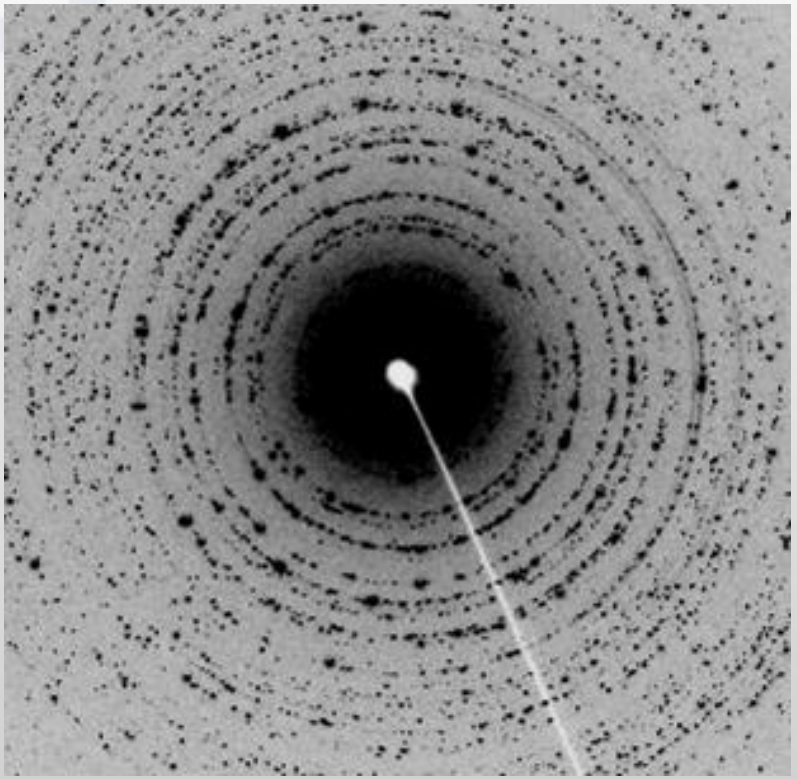

Make a powder into a bunch of single crystals we could index

1000 micron beam
+ turning

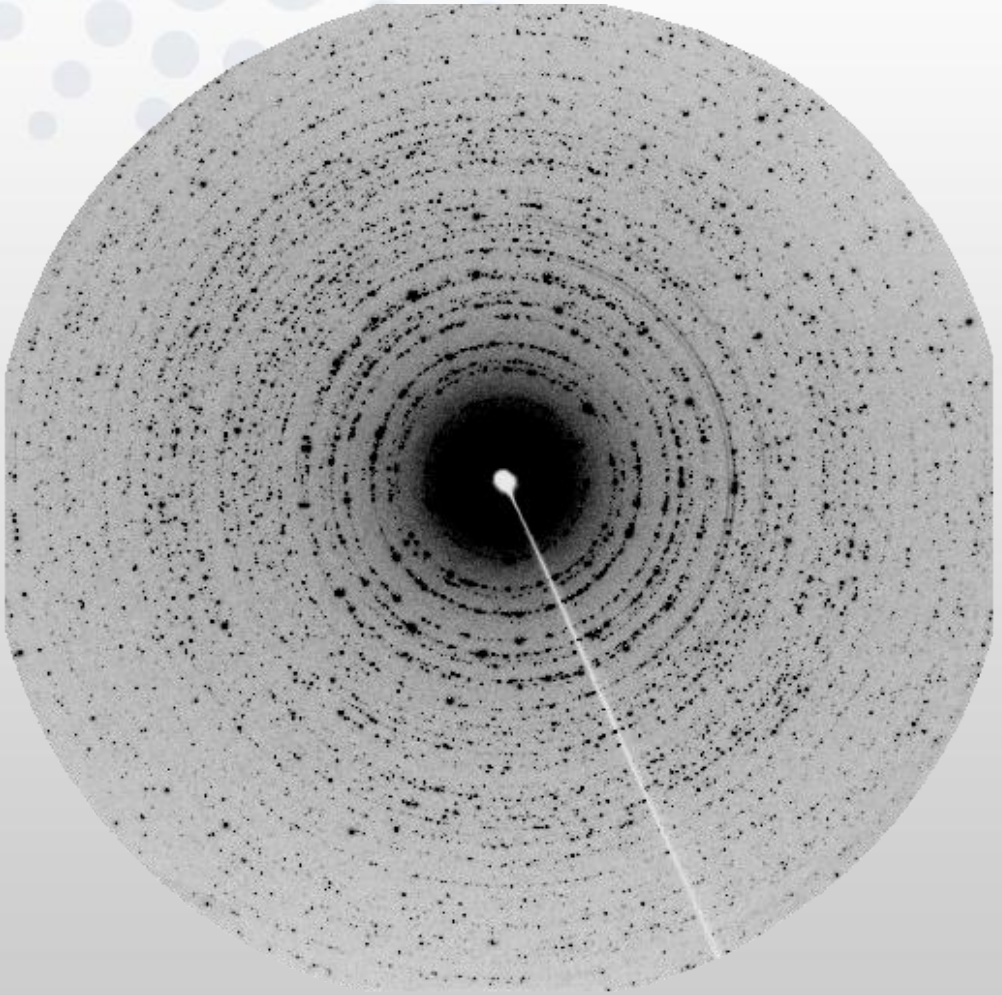

Make a powder into a bunch of single crystals we could index

1000 micron beam

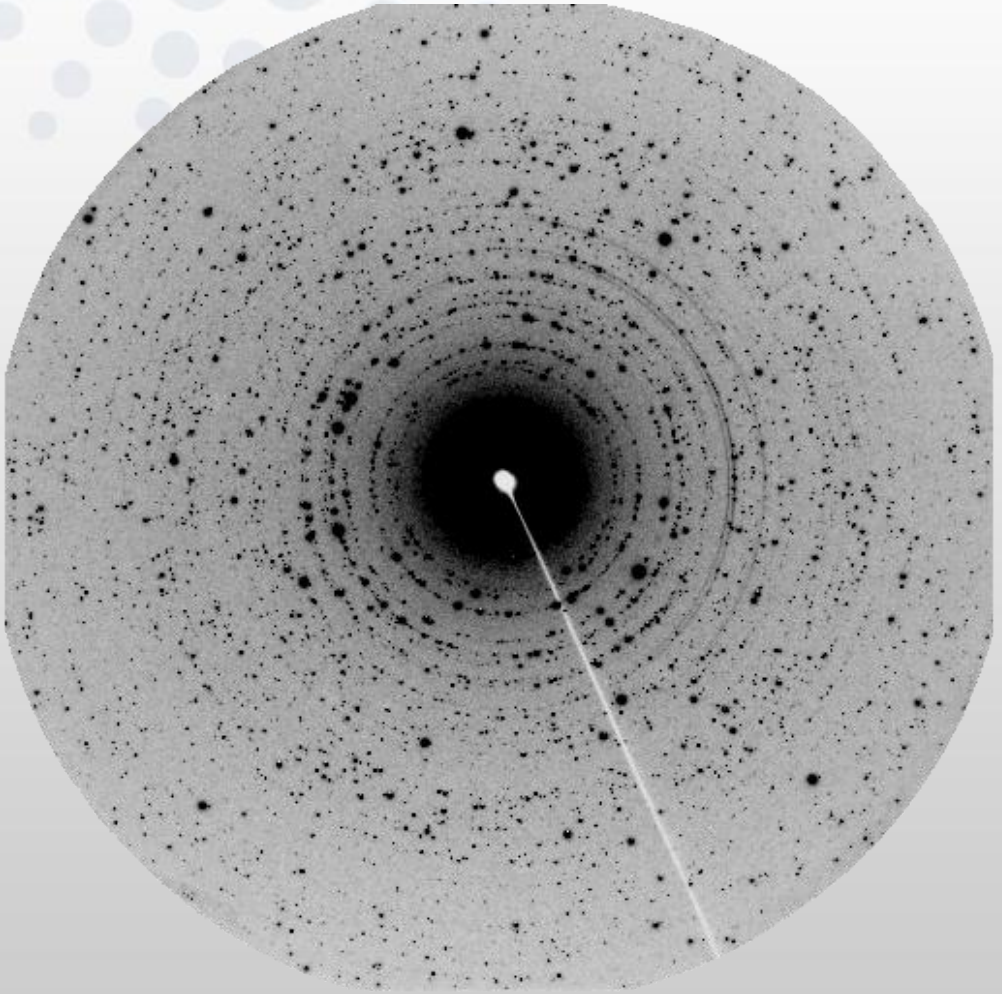

Make a powder into a bunch of single crystals we could index

900 micron beam

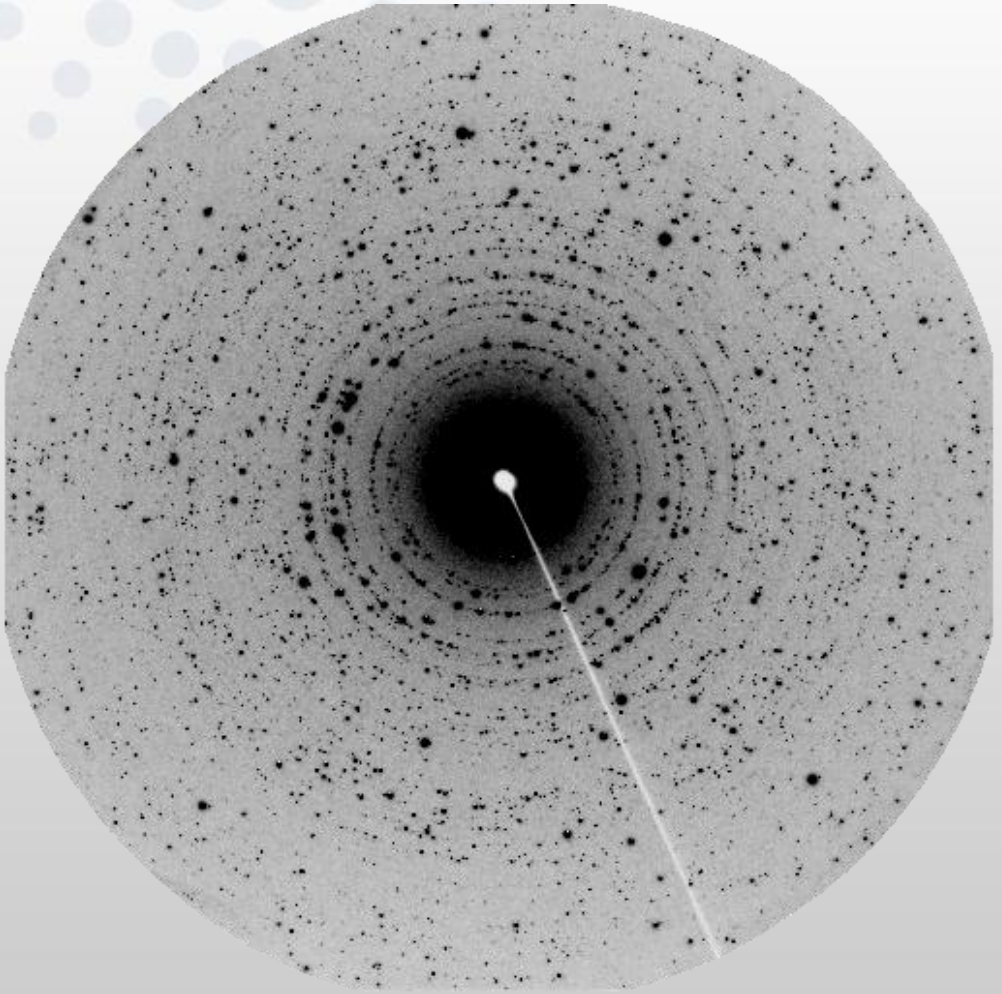

Make a powder into a bunch of single crystals we could index

800 micron beam

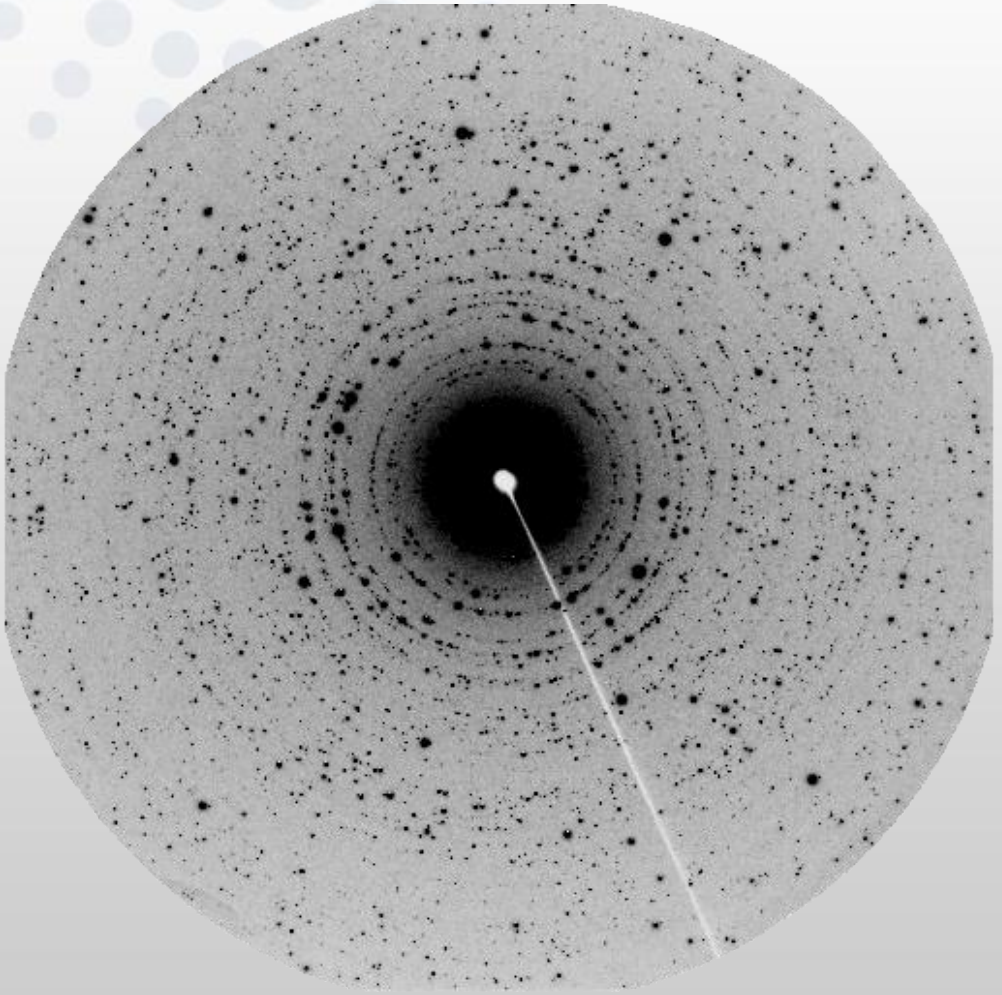

Make a powder into a bunch of single crystals we could index

700 micron beam

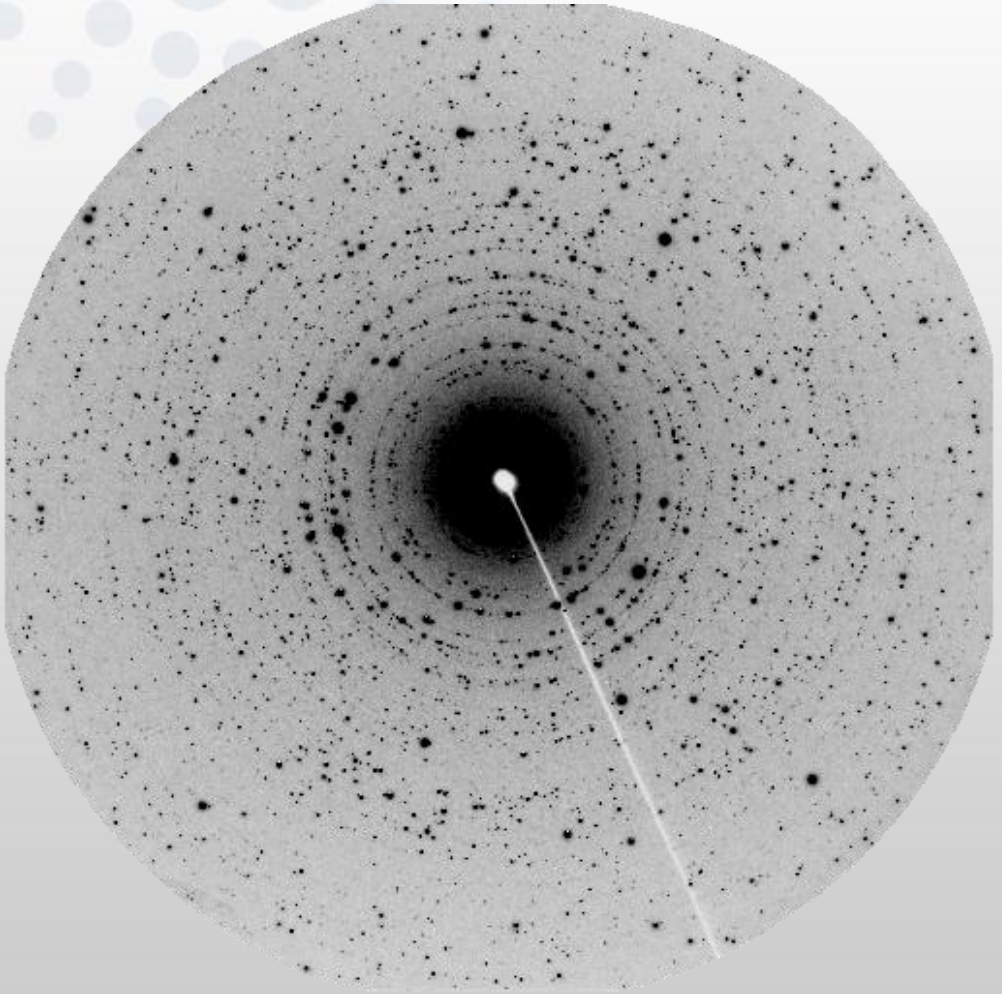

Make a powder into a bunch of single crystals we could index

500 micron beam

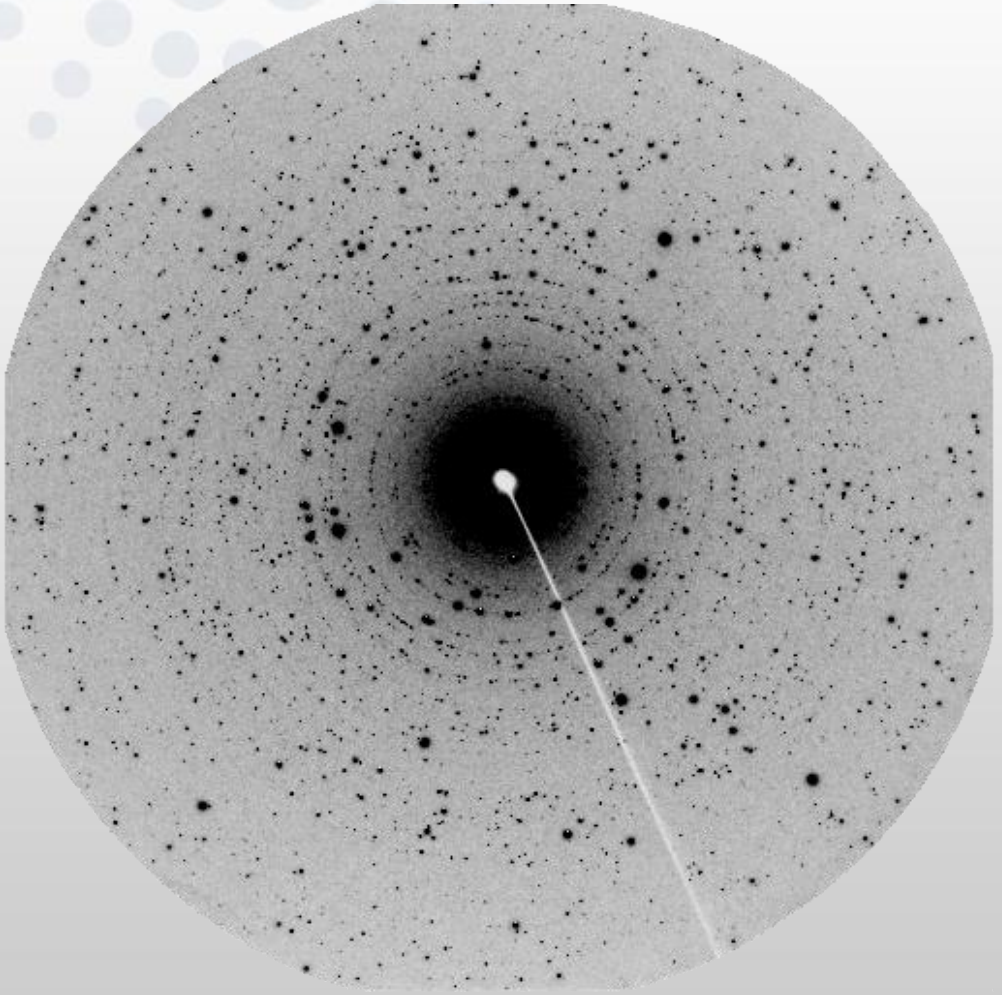

Make a powder into a bunch of single crystals we could index

400 micron beam

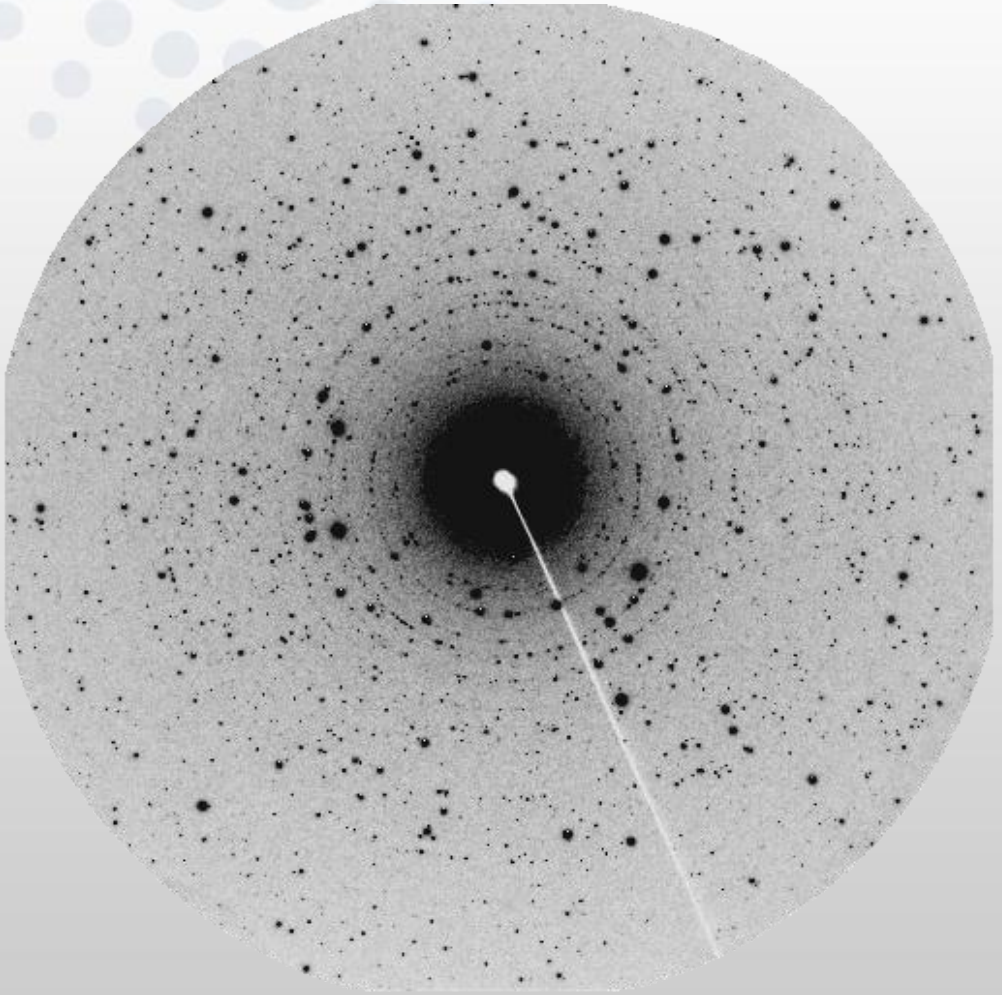

Make a powder into a bunch of single crystals we could index

300 micron beam

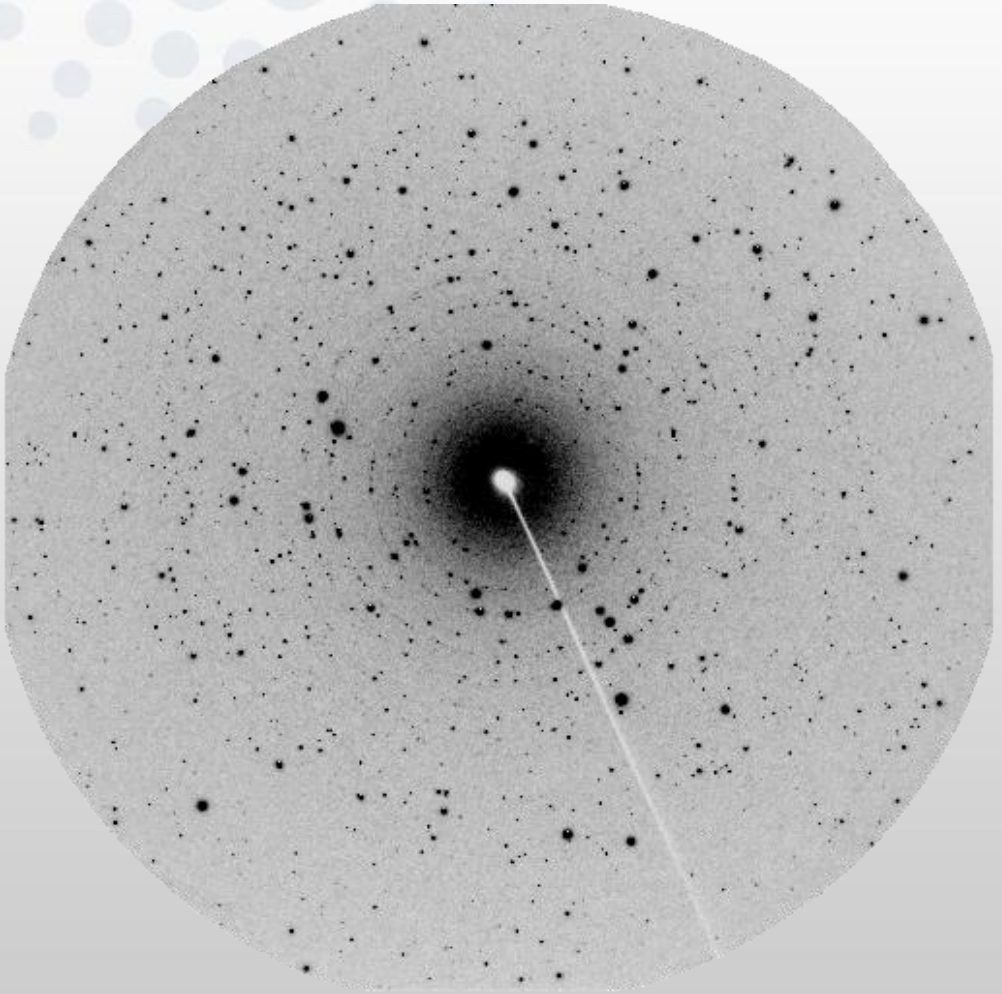

Make a powder into a bunch of single crystals we could index

200 micron beam

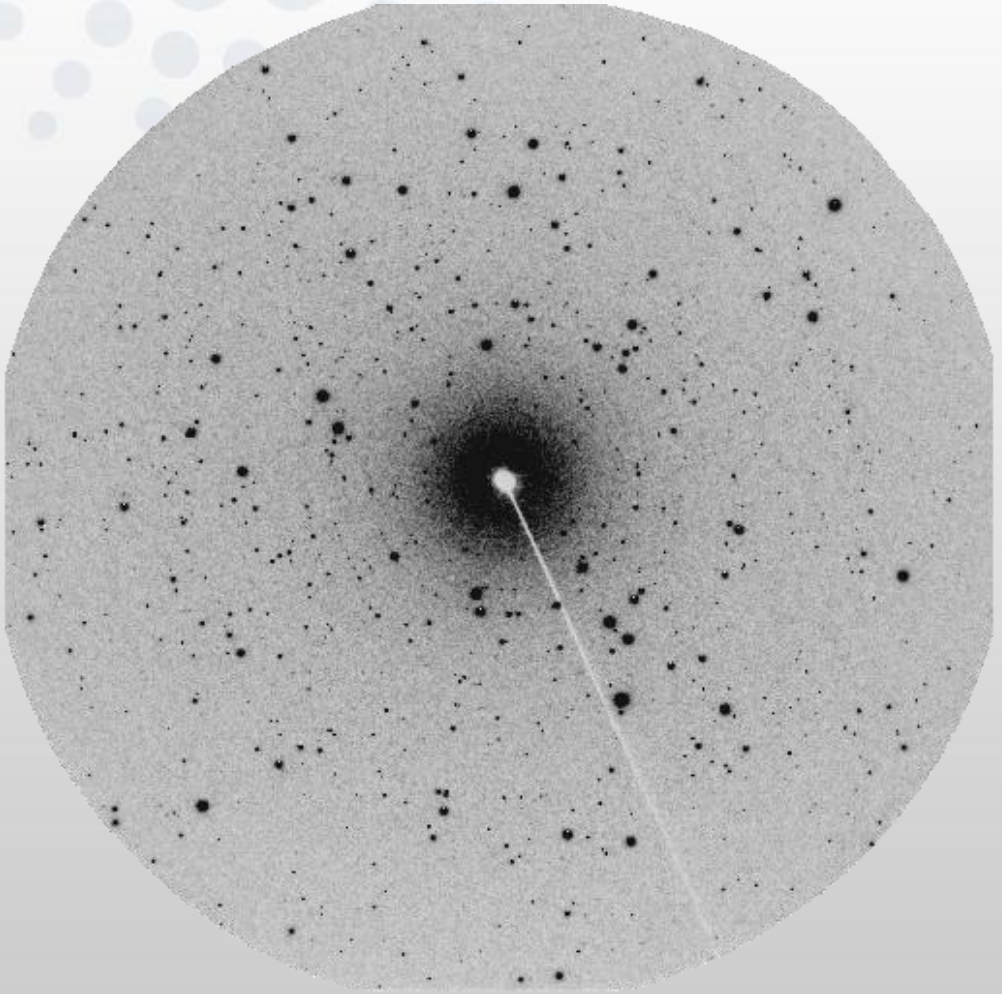

Make a powder into a bunch of single crystals we could index

100 micron beam

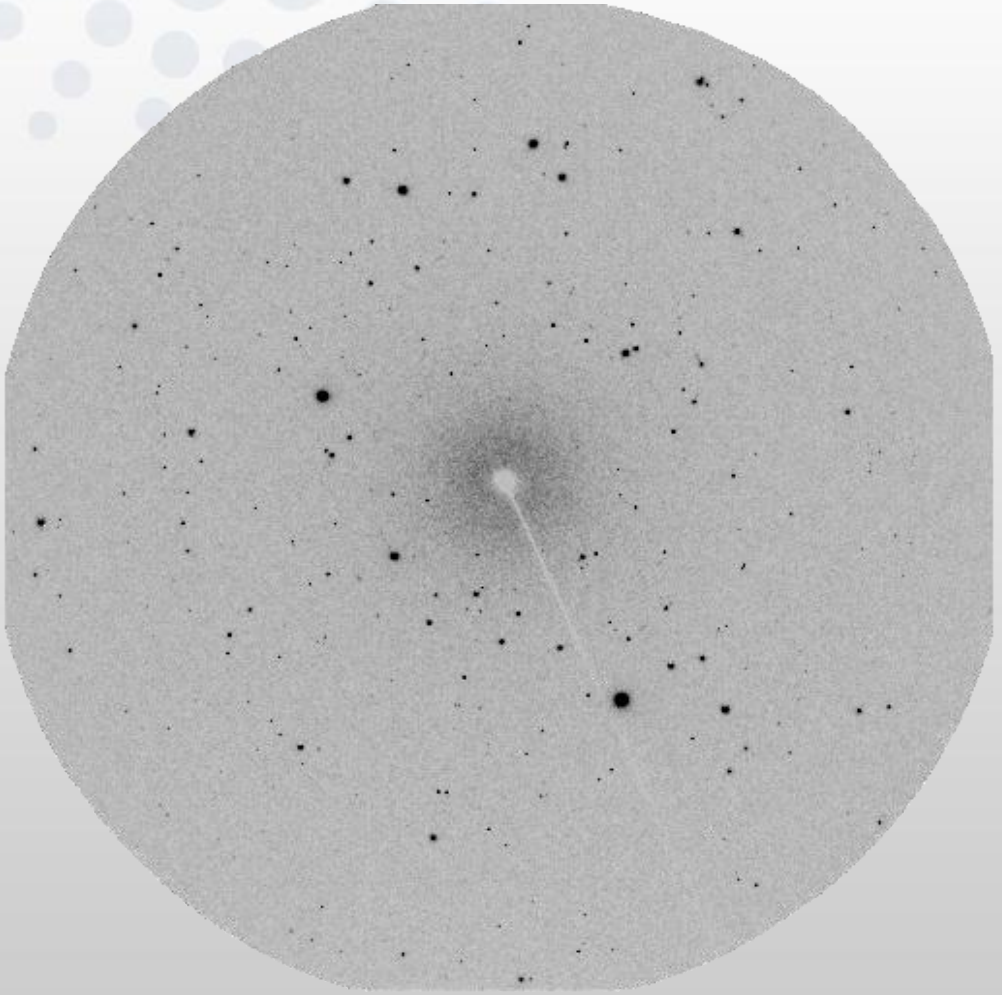

Make a powder into a bunch of single crystals we could index

50 micron beam

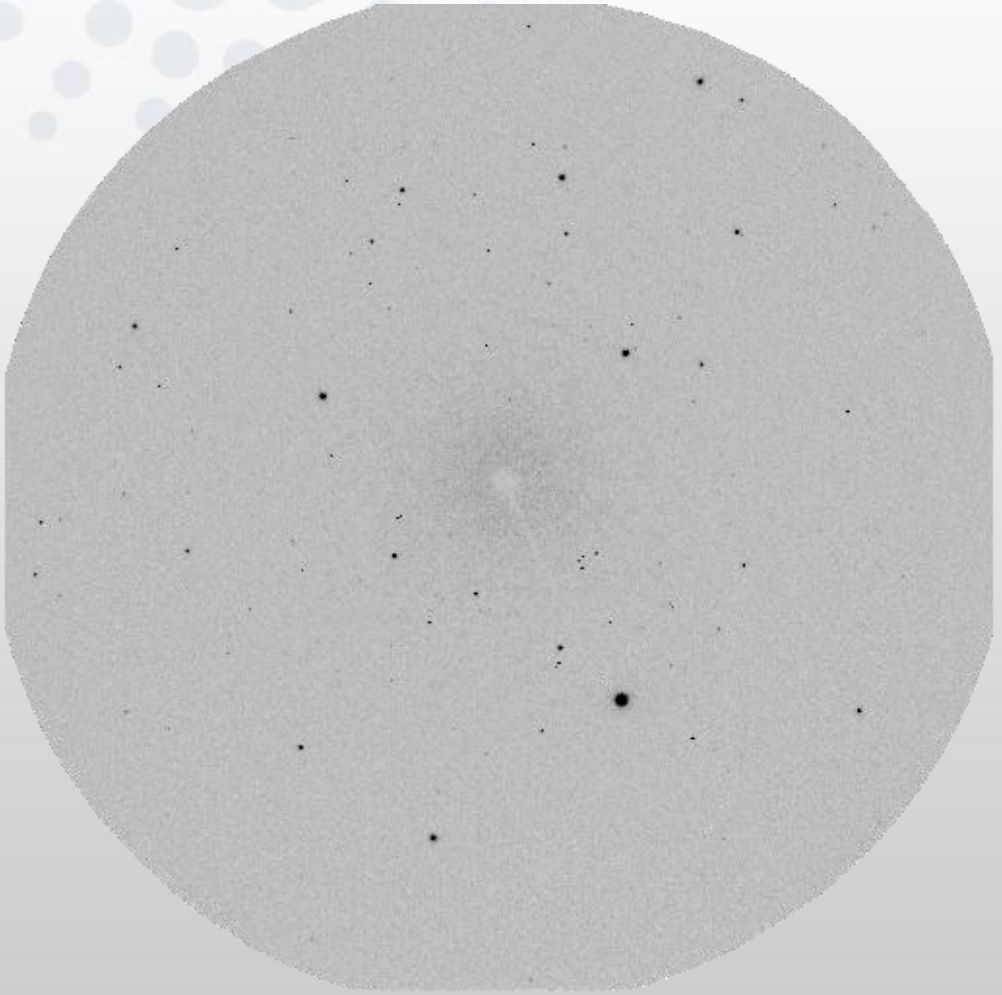

Make a powder into a bunch of single crystals we could index

30 micron beam

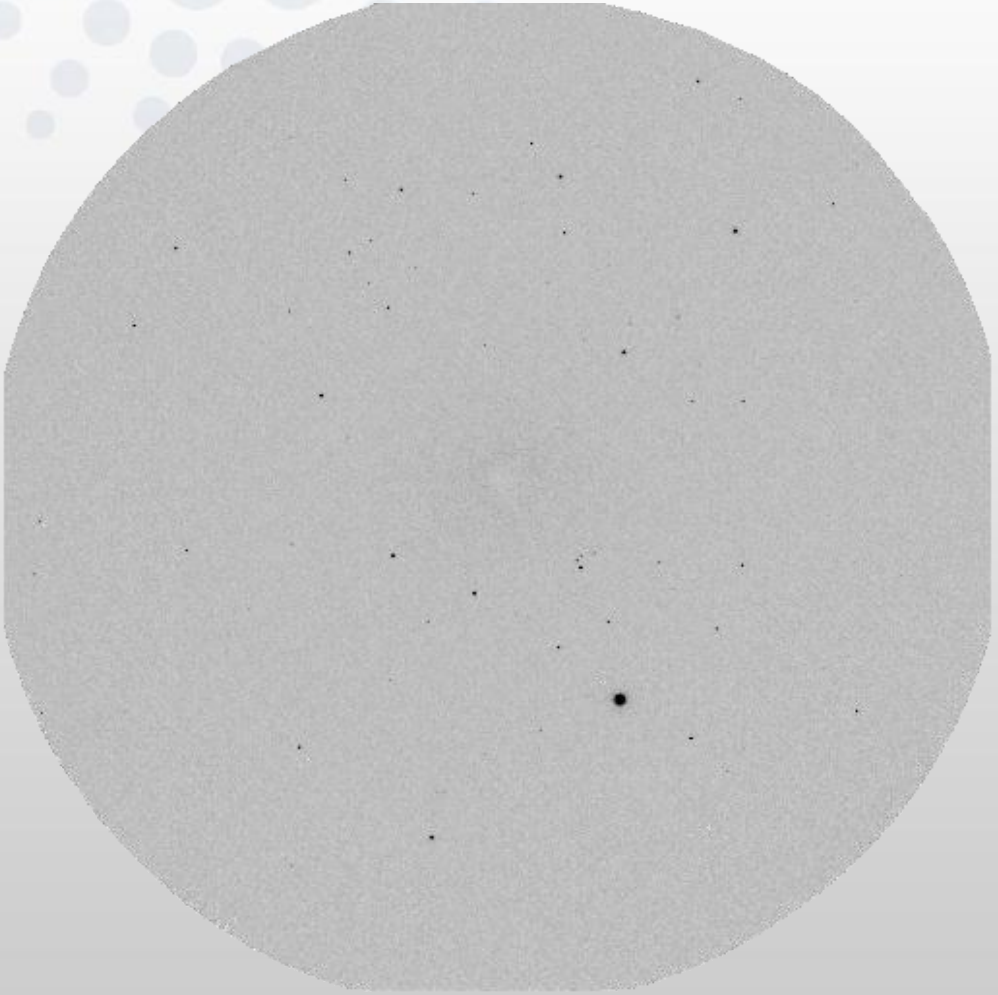

Determine grain centres and orientation matrices

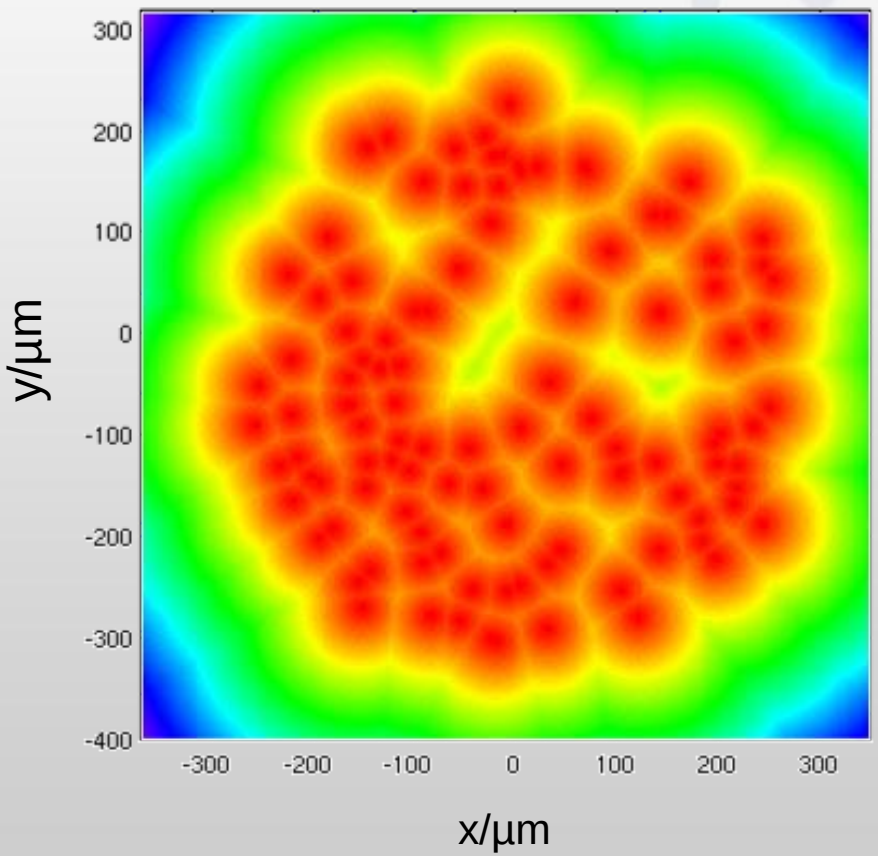

Grain positions, orientations, lattice parameters all simultaneously refined from low resolutoin multi-crystal data

"grain boundaries" from Voronoi calculation: if the grain centre falls in the middle of the reconstructed grain, perhaps nothing is missing.

Vaughan et al., in progress

Adding orientational information

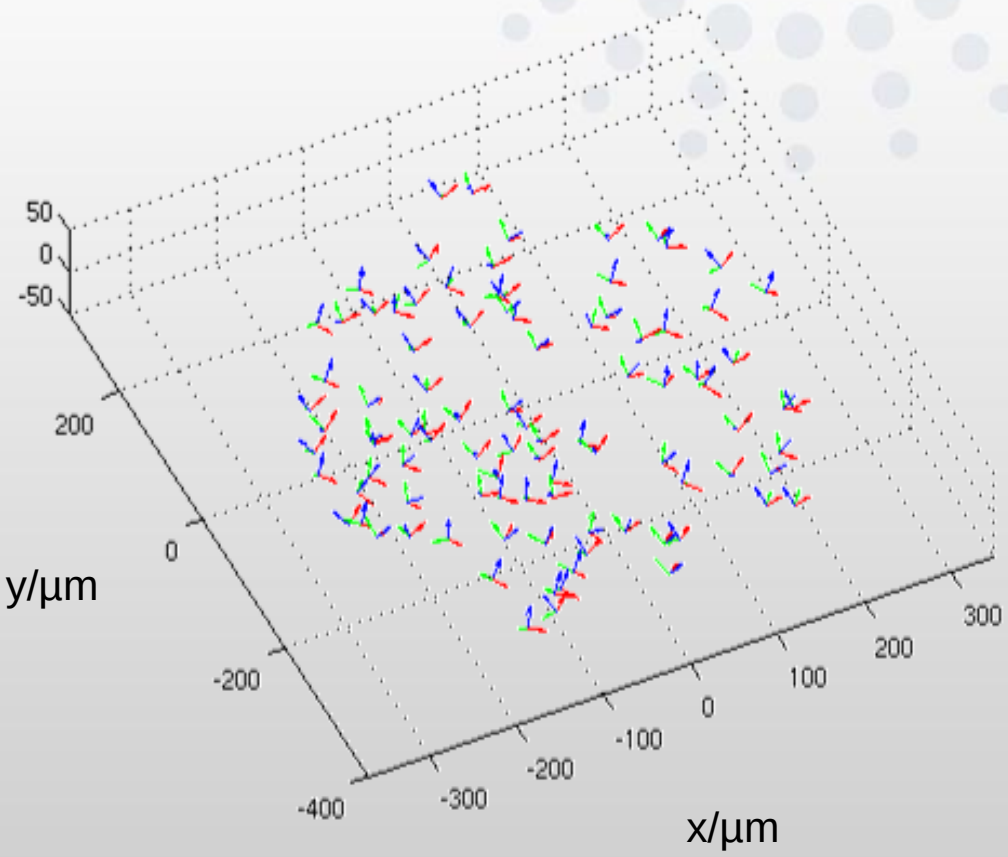

The axes are placed at the crystal centre (this is for one layer).

J. J.W. Morris et al., *Acta Materialia* (2010)

Rotations after each step

Depicted are the Rodrigues vectors of subsequent rotations after straining a sample

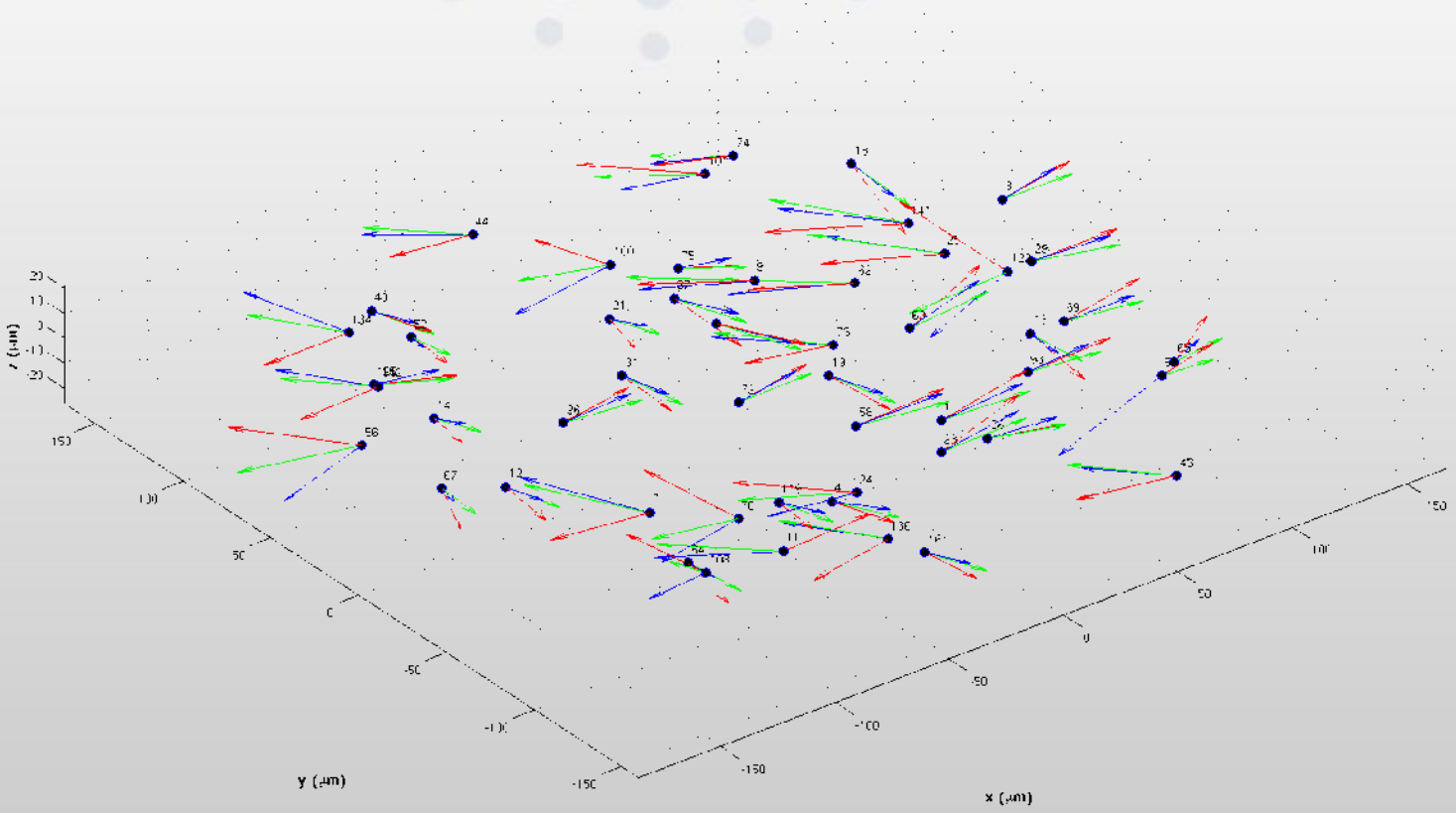

Layer by layer maps

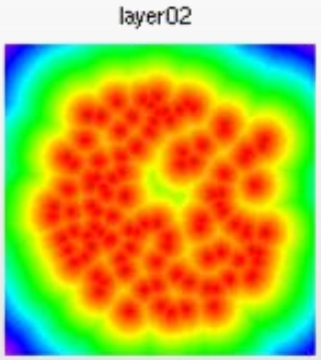

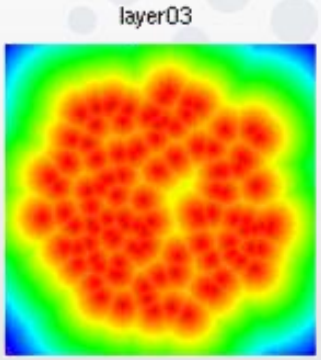

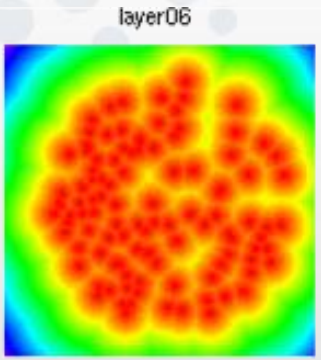

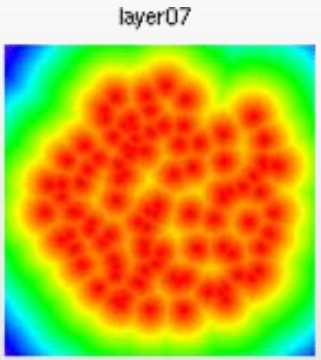

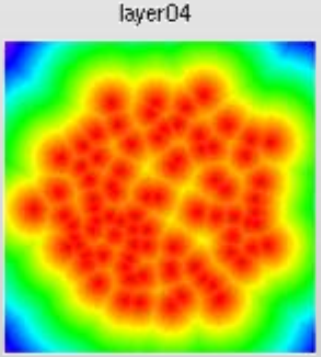

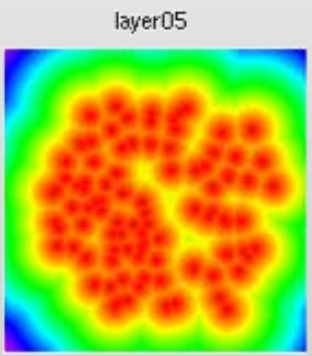

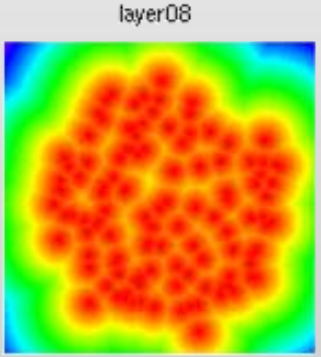

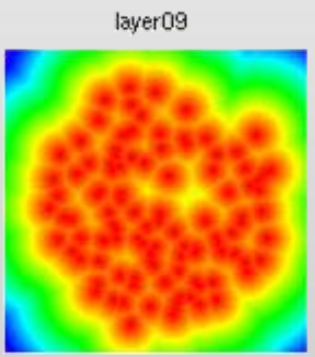

These are constructed using only grains with a match above and/or below

High Resolution Grain map

A combination of detectors allows the high resolution map to be constructed while we characterize simultaneously:

- Grain Shape
- Grain Position
- Crystal Structure
- Strain State

For each crystal independently

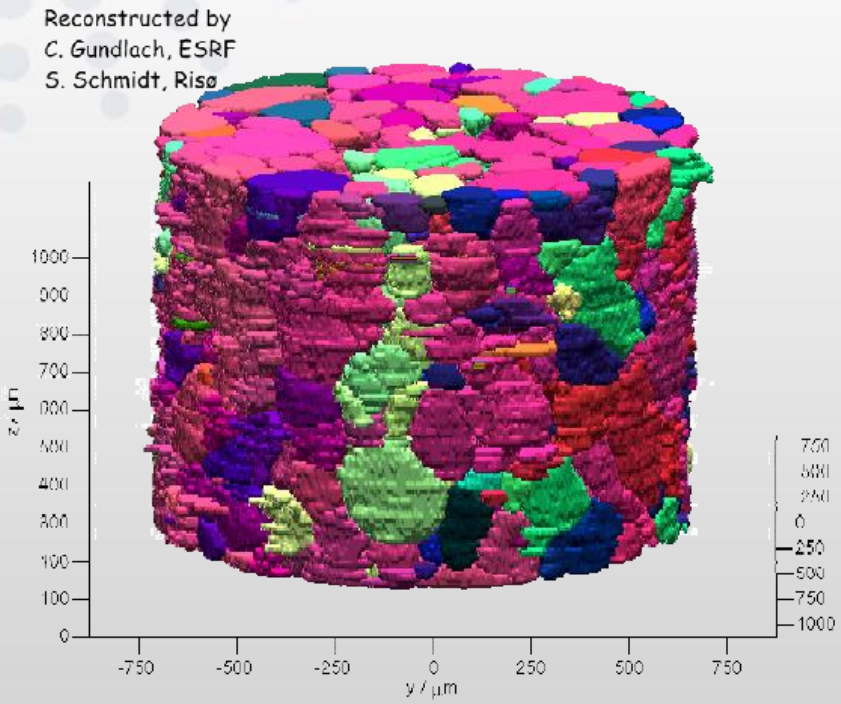

Schmidt et al., Science (2007)
Gundlach et al., in progress
Juul Jensen et al, Materials Today(2006)
Vaughan et al (2010)
Poulsen et al (2010)

Diffraction Contrast Tomography (ID11)

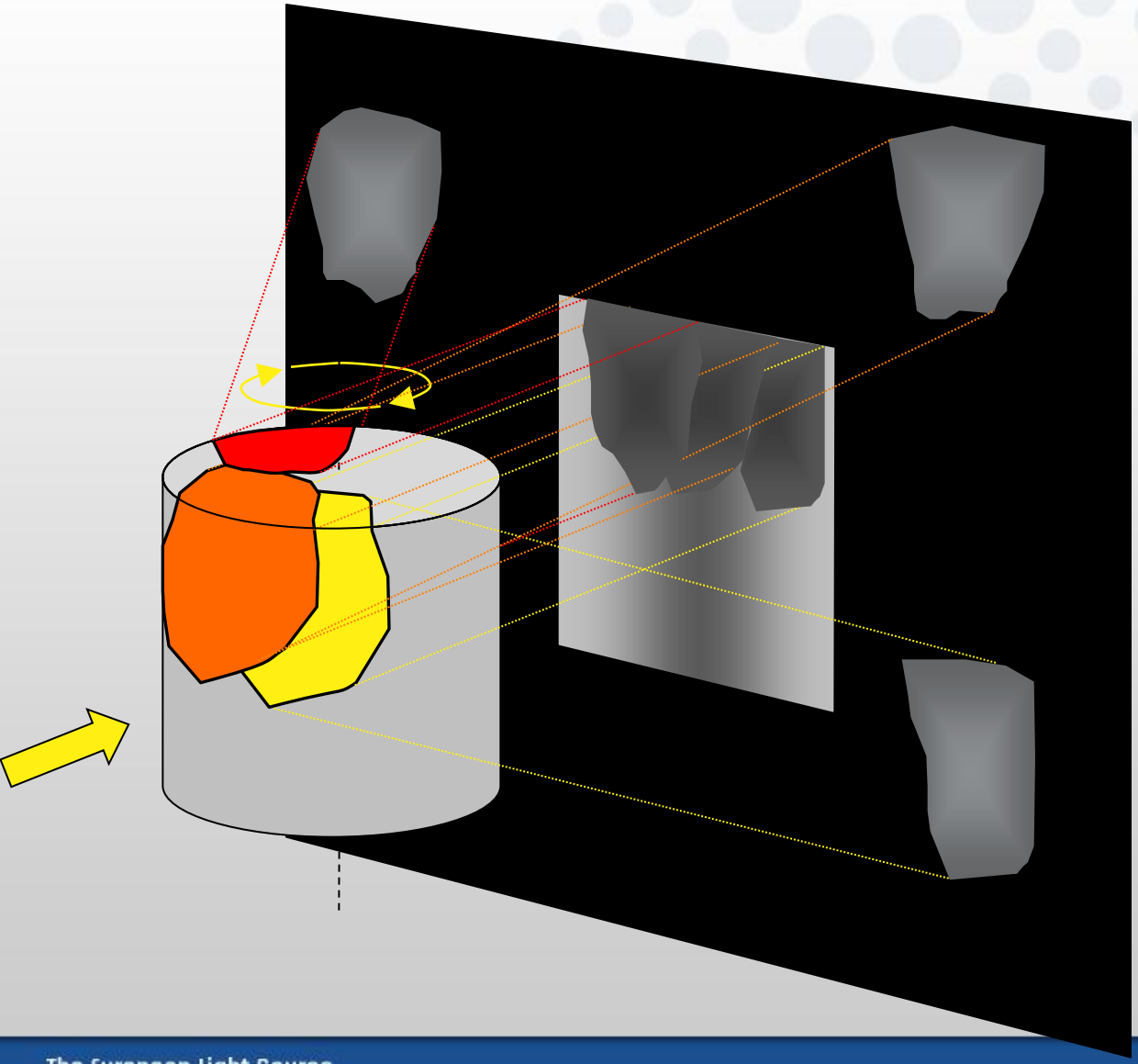

Acquisition of both the diffraction and extinction data allows the measurement of grain distributions, orientations and strain state in materials without density contrast

Diffraction Contrast Tomography

Algebraic reconstruction methods allow the calculation of 3 dimensional grain maps with micron-level precision – resolution is determined currently by detectors

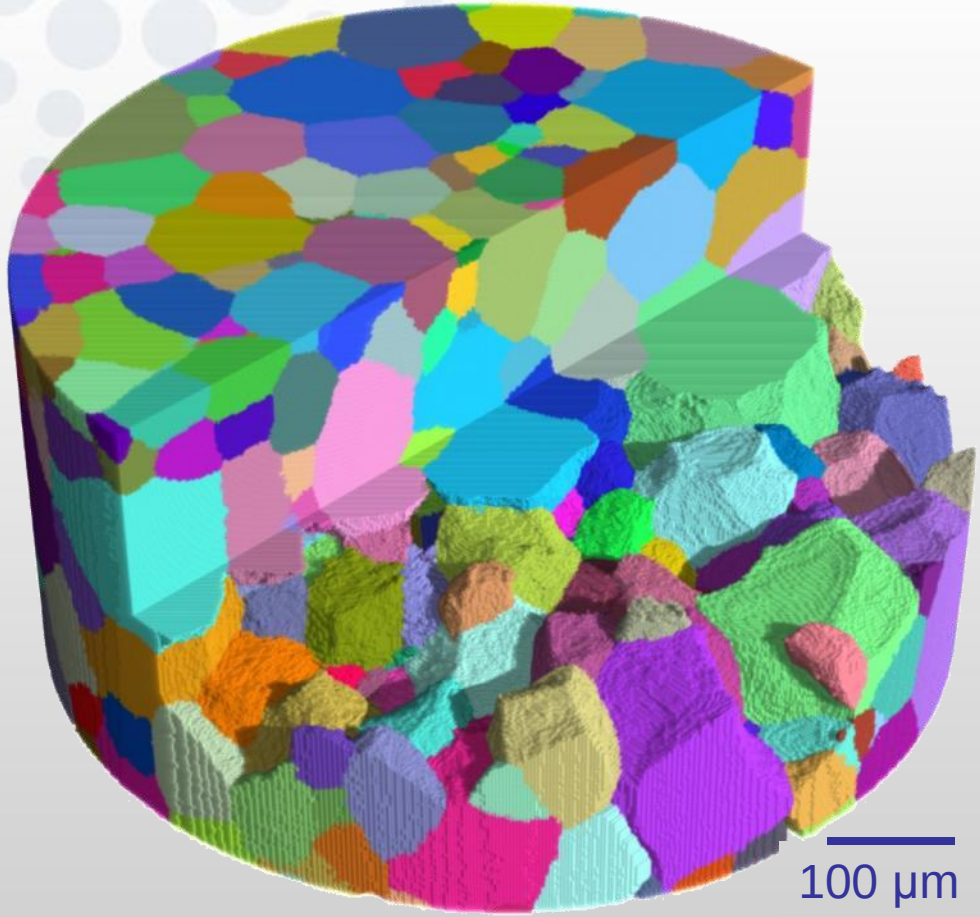

W. Ludwig et al., *Rev. Sci. Instrum.* (2009)

Combining Grain Mapping with Tomography

Grain map from diffraction contrast tomograph to identify grain shapes and orientations

Conventional tomograph to identify crack

To relate crystal orientations to crack propagation

Collaboration between Manchester University and ESRF

A. King, et al., *Science (2008)*
G. Johnson, et al., J. Appl. Cryst. (2008)

Improving resolution of map with microscopy

There are not any good tricks to improve the resolution of the diffraction, but imaging can be improved magnifying the projections.

Aim: Reconstruct grain map from far/near field diffraction data

Refine map with magnified DCT extinction data and/or "normal" tomography data from very distant detector

Diffraction/ Full-Field Nanoscopy Setup

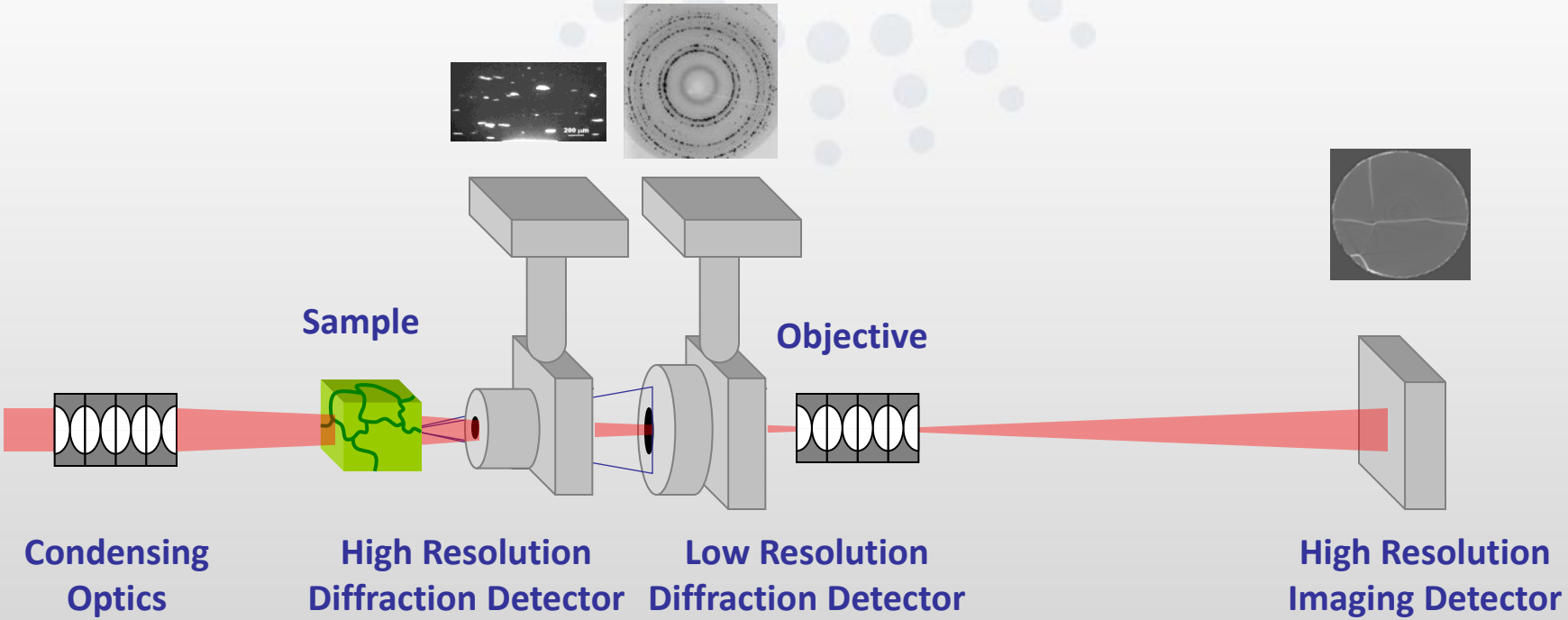

Lensless Microscopy (ID01,ID10)

1. CDI from single objects

Shape and strain of single nano-objects. Beam larger than sample.

2. Holographic approach

Phase encoded in the diffraction amplitude: no need for inversion algorithms. Beam larger than sample.

Phys Rev Lett **104** 165501 (2010)

3. Ptychographic approach

Redundance of information from overlapping areas. Reconstruction of sample *and* probe. Beam smaller than sample.

Nature Commun. ***2*** 568 (2011)

4. Wave-front investigation

The knowledge of the x-rays probe used for each experiment.
Disentangling contributions from sample and probe
More accurate determination of phase

Optics Express ***19*** 19223(2011)

Mathematical algorithms ?

$$I(\vec{q}) = \left| FT\left\{ \rho(\vec{r}) e^{i\Phi(\vec{r})} \right\} \right|^2 = \left| F(q) \right|^2$$

Real Space

Reciprocal Space

$G(r) = \rho^C(r) e^{i\Phi^C(q,r)}$

FFT

$F^N(q) = f(q) \bullet e^{i\phi^N(\vec{r},q)}$

I^M Measured intensity

Finite support condition

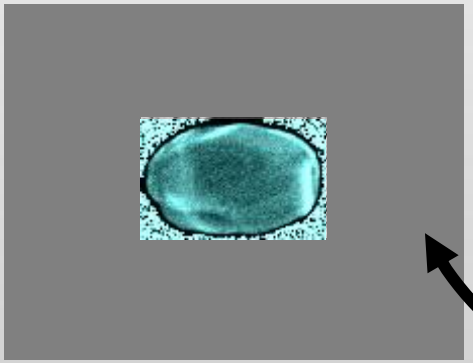

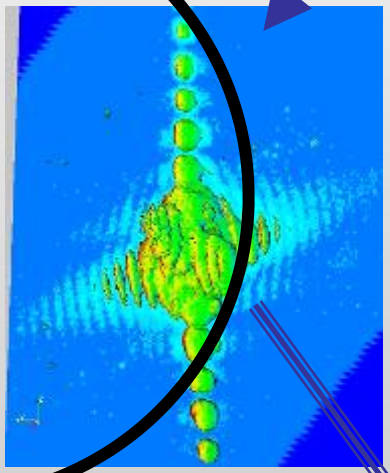

+

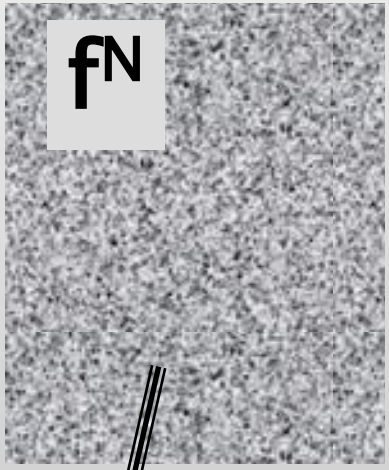

$G(r) = \rho^R(r) e^{i\Phi^R(q,r)}$

FFT^{-1}

$F^N(q) = \sqrt{I^M(q)} \bullet e^{i\phi^N(\vec{r},q)}$

3D reconstruction

- Inversion of the 3D intensity matrix in a *single* inverse Fourier Transform

- Plot of the 3D object in an orthogonal space

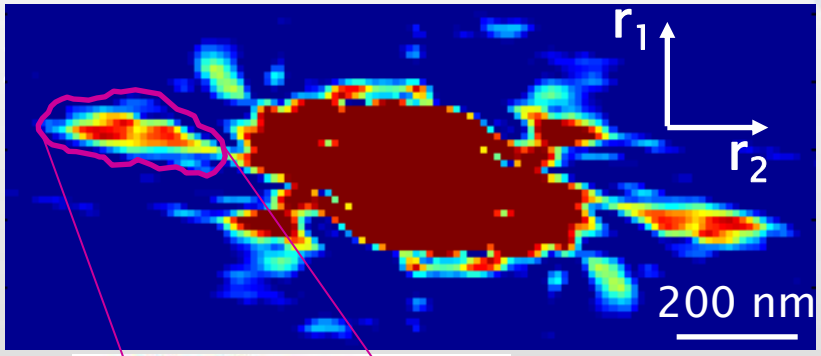

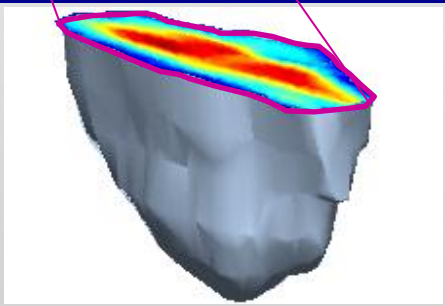

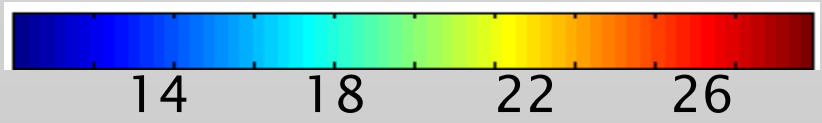

(a)

(c)

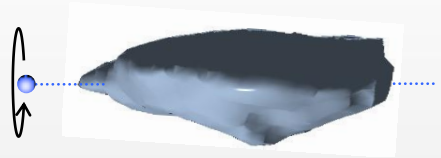

200 nm

Comparison with AFM

(b)

(d)

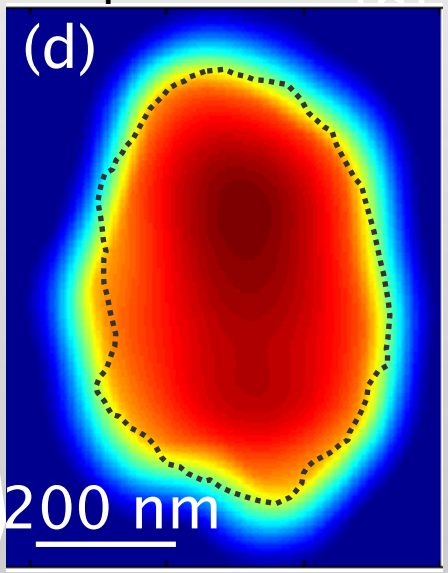

Ptychography: use of redundancy

Measurement of several diffraction patterns obtained for different but overlapping illumination areas

$$y(\mathbf{r}, \mathbf{R}) = O(\mathbf{r} - \mathbf{R}) \times P(\mathbf{r})$$

$O(\mathbf{r})$ the *object function*,
$P(\mathbf{r})$ the *illumination function*
$y(\mathbf{r})$ the exit wave,
$\mathbf{R}$ the displacement of the beam

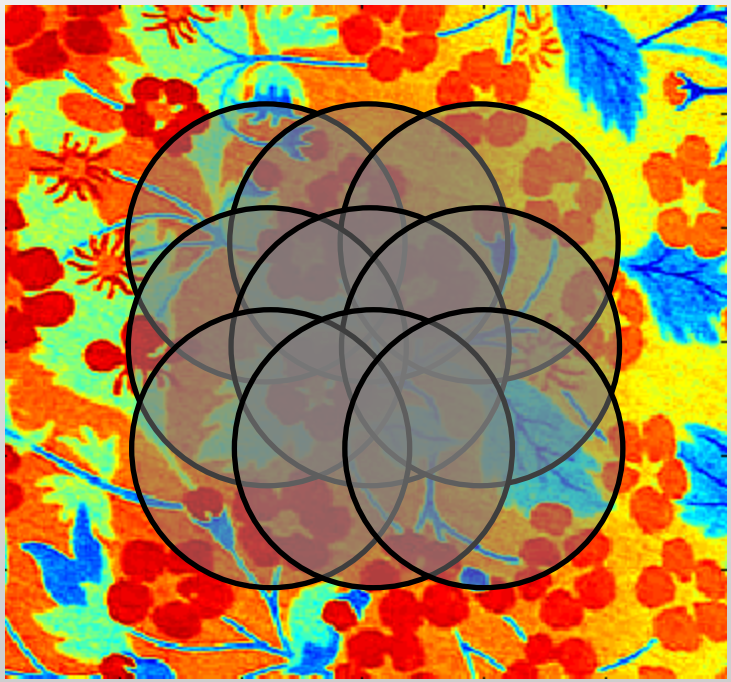

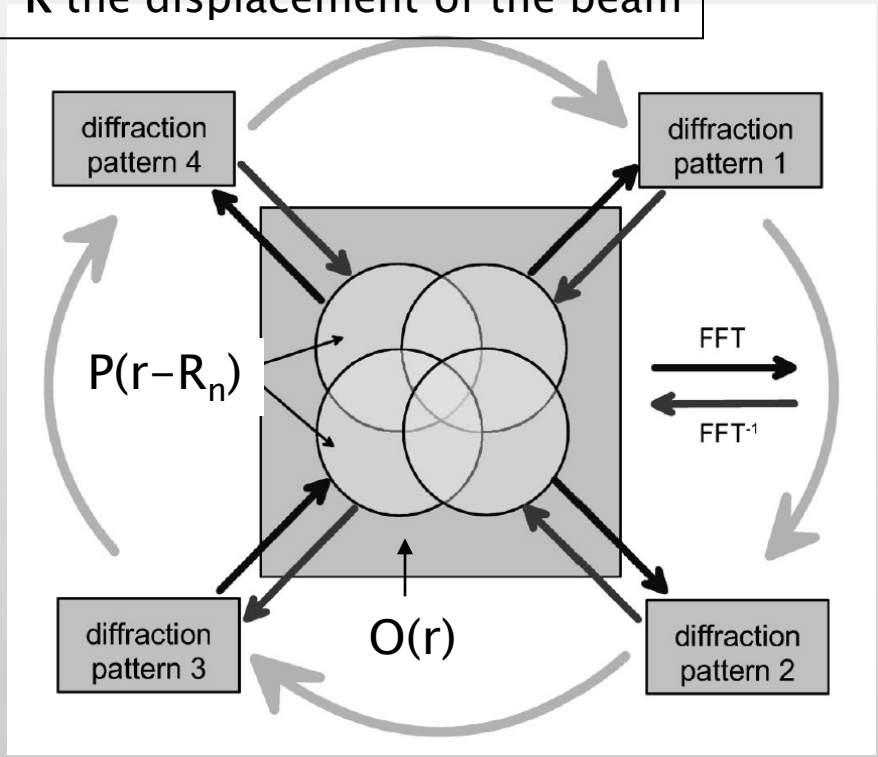

*Faulkner et al. PRL **93** (2004); Rodenburg et al. APL **85** (2004)*

Allow Total Characterisation

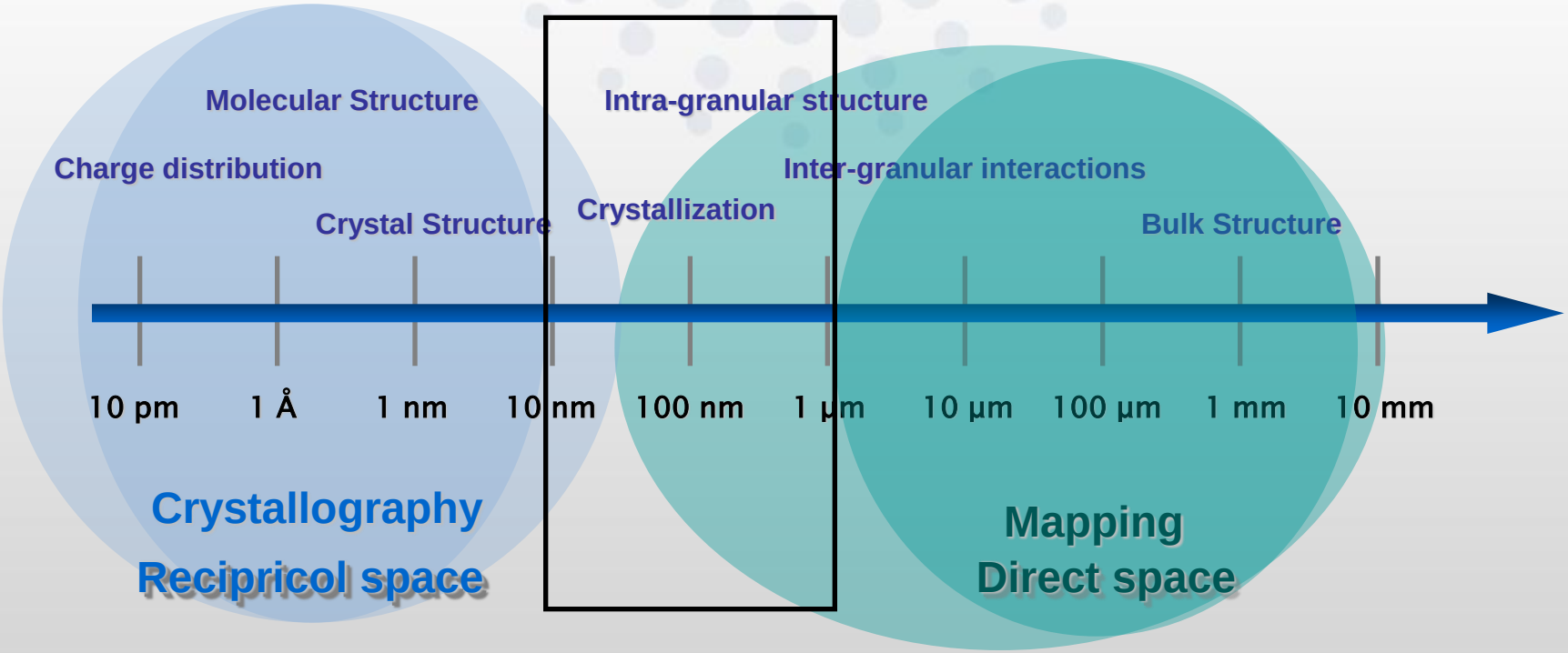

New Science

Thanks for slides and support

Dina Carbone (ID01)
Tobias Schulli (ID01)
Roberto Felici (ID03)
Andy King (ID11)
Wolfgang Ludwig (ID11)
Marco Di Michele (ID15)
Andy Fitch (ID31)

ESRF Structure of Materials

Surfaces, Interfaces and Bulk

Techniques: X-ray Diffraction, Scattering, Imaging, etc.

ID01	ID03	ID15	ID11	ID31
Tobias Schulli	Roberto Felici	Veijo Honkimaki	Gavin Vaughan	Andy Fitch
Surface diffraction		Buried interfaces Liquid surfaces Bulk diffraction Fast tomography	Nano beams Grain mapping DCT Chemical crystallography Fast powder diffraction	High resolution powder diffraction 6 – 62 keV
Coherent diffraction imaging Nano beams	Catalysis			